Heinz Langhals[1]

Fluorescence and fluorescent dyes

[1] Department of Chemistry, Ludwig-Maximilians-Universität, Butenandtstr. 13, Munich D-81377, Germany, E-mail: Langhals@lrz.uni-muenchen.de

Abstract:
The handling and control of light is becoming more and more attractive in science and technology such as data processing and requires functional chromophores. As a consequence, fluorescent materials are of special importance because they allow the processing of light energy. Thus, basics of fluorescence are reported as prerequisites for planning complex functional structures. Various fluorescent systems are presented beginning with historic observations followed by a detailed discussion of light absorption and emission indicating fluorescent chromophores as molecular resonators; molecular dynamics and intermolecular interactions are leading to complex functional materials.

Keywords: fluorescence, chromophores, optical functional materials, light emission, molecular dynamics
DOI: 10.1515/psr-2019-0100

1 Introduction

Fluorescence, the spontaneous light emission of irradiated materials was empirically found. Linen weavers in the seventeenth century noticed brilliant purely white shades of garments after treatment with extracts of horse chestnuts where fluorescence caused optical bleaching. The background of this effect was not clear at that time. The pharmacist W. Raab [1] described special optical effects of such extracts where the active compound Aesculin (RN 531-75-9) was further investigated by F. Rochleder and R. Schwarz [2] and reported by Berzelius [3]. However, there was still minor interest in such organic materials. More attractive for chemists were shiny minerals such as uranium ores. Further progress brought about the development of new and systematic methods in organic chemistry in the middle of the nineteenth century by chemists such as Adolf von Baeyer. He developed Fluorescein (see below) as a synthetic organic material forming impressively fluorescent aqueous solutions in daylight. There were only rare applications of fluorescent materials in the beginning [4] such as tracer experiment for the detection of streams of ground-water; the photostabiliy of the first optical whitening agents was low restricting their general application. Moreover, the majority of organic compounds are not fluorescent so that a search for such special classes of compounds delayed the further developments where the mostly limited photostability was an important obstacle. Meanwhile, the chemistry and physics of fluorescent dyes are well developed with numerous applications in an increasing field such as optical whitening agents for paper, textiles and various other white or bright materials where the impressive optical effect of fluorescence is not only of interest for marking inks, but also for safety wear and signage, but also for security printing and leak proofing. The temporary storage of light energy forms the basis for dye lasers and the spontaneous light emission is important for OLEDs. The green fluorescent protein brought about an appreciable progress in biochemistry. Applications and further developments of fluorescent materials are favored by the knowledge of the interaction of light with matter. Thus, the interaction of light with matter obtains an increasing importance both in science and technology. Visible light is electromagnetic radiation with frequencies in the range between 0.4 and 0.8 PHz; see Figure 1. Thus, the molecular handling of light may be named petahertz technology [5].

Heinz Langhals is the corresponding author.

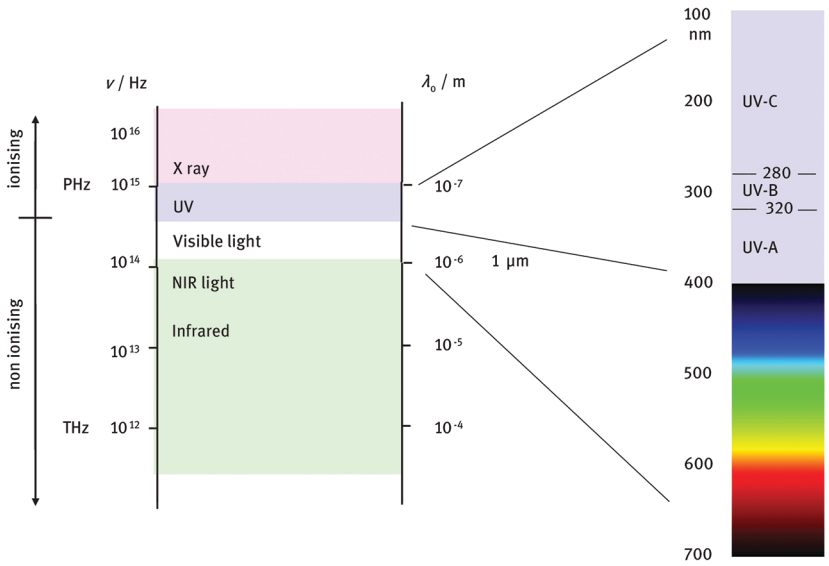

Figure 1: Significant regions of electromagnetic radiation for fluorescence. Left scale: Frequency, right scale vacuum wavelengths.

Visible light is usually characterized by the vacuum wavelength λ_o in nm with the velocity of light c according to eq. (1) (the velocity of light in vacuo c_o for λ_o) because of historic measurements by means of optical grids; see Figure 1. A further common measure is the wavenumber $\tilde{\nu}$.

$$v = c/\lambda = c \cdot \tilde{\nu} \tag{1}$$

The energy E of radiation is not continuously absorbed by matter, but in small quanta according to Einstein's Formula (2) where h is Planck's constant, c is the velocity of light, ν is the frequency and λ is the wavelength.

$$E = h \cdot v = h \cdot c/\lambda \tag{2}$$

The absorbed energy E may induce various chemical processes; thus, the frequency ν in cps or the proportional wavenumber $\tilde{\nu}$ (in cm^{-1} known as Kayser K or the multiple unit kK) are more clear in chemistry where energetic processes are dominant. However, wavelengths λ are mostly reported where one has to keep in mind that they are the inverse of energy.

2 Elastic and inelastic interaction of light with matter

$$\mathbf{n} = n - i \cdot \kappa \tag{3}$$

A continuous model of the electromagnetic field describes sufficiently precisely the interaction of propagating electromagnetic waves with matter in macroscopic dimensions and comparably low frequencies such as for radio transmitters [6]. A propagating electromagnetic wave induces more or less damped oscillations where a complex index of refraction $\mathbf{n}$ in eq. (3) is an appropriate description. The real component n represents the contribution to the optical index of refraction and the imaginary κ a linear measure of the absorptivity.

Thus, n represent elastic interactions with matter without loss of energy and κ inelastic interactions with the absorption of the radiation. The dependence of the parameters n and κ on the frequency ν can be calculated by means of classical electrodynamics and results in Formula (4) where ν_o means a resonant frequency of matter and γ characterizes the aptitude for light absorption; a and b combine mathematical and natural constants and a proportionality factor concerning the dimension of ν.

$$\mathbf{n} = a \cdot \frac{v_o^2 - v^2}{(v_o^2 - v^2) + \gamma^2 v^2} - i \cdot b \cdot \frac{\gamma v}{(v_o^2 - v^2) + \gamma^2 v^2} \tag{4}$$

Multiple resonances ν_o require a sum of individual terms according to eq. (4).

The wavelengths of light of about 500 nm extends to macroscopic dimensions just below 1 μm [7]; the molecular components of matter are appreciably smaller and thus, can be considered as homogeneous media where eq. (4) describes the interaction with sufficient precision. The calculated spectral dependence of the contribution to the index of refraction n characterizing the elastic light scattering is reported in Figure 2 (dashed curves), top for a scale linear in energy and in Figure 2, bottom more familiar for linear in wavelengths λ. The index n exhibits maxima and minima in the region of resonance, however, changes monotonously off-resonance. Colorless materials absorb light in the UV below 400 nm, but are transparent in the visible. As a consequence, the index of refraction is high for short wavelengths such as for blue light (compare the right dashed branch in Figure 2, bottom) and decreased for longer wavelengths such as for red light; this is known as normal dispersion and is applied in dispersing optical components such as prisms. A completely different spectral dependence is observed if light is absorbed in the visible shown in Figure 2 (dashed curves) where there is a reverse of the index of refraction known as anomalous refraction; the gem tourmaline is the most prominent example for such an optical behavior. Such anomalous dispersion in the visible causes an unusual sequence of color for the refraction of white light. The appendant absorption spectrum calculated from κ resembles a Lorentz curve (Agnesi curve) and is shown in Figure 2, dotted curves. A comparably slim maximum of κ and appreciable tailing to shorter and longer wavelengths can be seen; the points of inflection of κ are close to the maxima and minima of the index of refraction n and the maximum close to the zero pass.

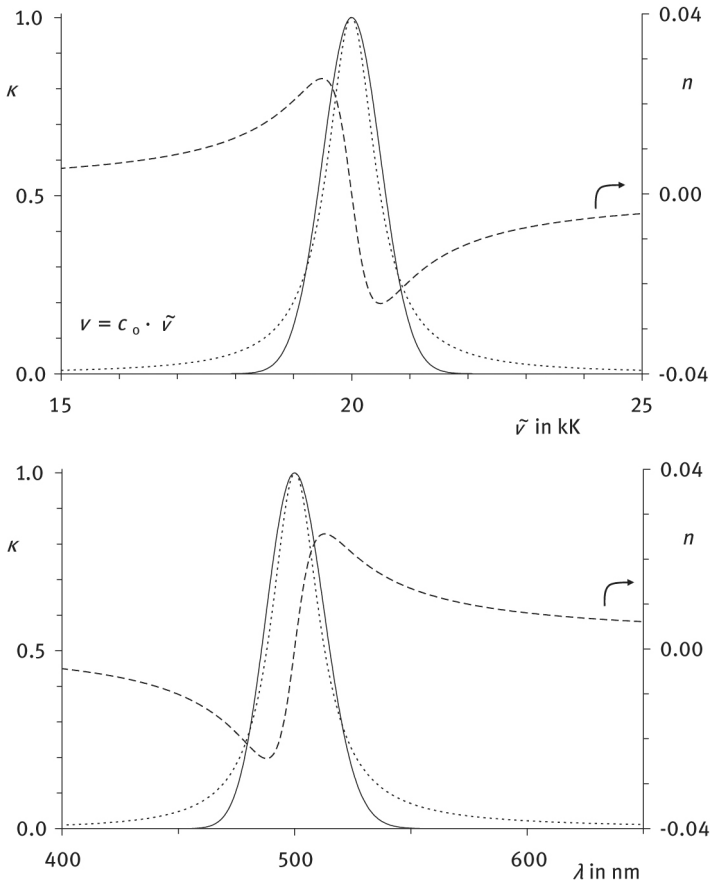

Figure 2: Normalized spectral dependence of the calculated absorptivity κ (dotted curves) and the contribution n to the index of refraction (dashed curves) compared with a Gaussian curve for absorption (solid curves). Top: Linear in wavenumber $\tilde{\nu}$ (proportional to the frequency ν) bottom: Linear in the wavelengths λ.

A homogeneous and isotropic medium would be required for the realization of a suitable continuous process; however, the resonators for visible light are local microscopic in their molecular dimensions and individually stochastically operating. The absorption (κ) is controlled by the transition probability being maximal at the resonance frequency and more and more lowered off resonance. This means a scattering in energy around the maximum depending on various other degrees of freedom such as by coupling with translation and libration vibrations in condensed phases, respectively. Such a distribution of multiple contribution of individually influenced stochastic processes results typically in a Gaussian dependence in energy and thus, in the electronic transition probability is best represented [8] in eq. (5), middle for multiple resonances n where $E_{(\nu,\lambda)}$ is the absorptivity proportional to κ depending of the frequency ν. $E_{\max(i)}$ are the maximal absorptivities of the individual Gaussian bands i, $\nu_{\max(i)}$ the positions and $\sigma_{(i)}$ the half widths. The inverse of the frequency ν must

be applied for the wavelength λ, Formula (5), right [9], where the factor 100 simplifies the interconversion between the wavelengths in nm and the wavenumbers in cm^{-1}. (Other functions such as the Lorentzian [10] or log-normal function are less appropriate for the description of experimental spectra).

$$E_{(v,\lambda)} = \sum_{i=0}^{n} E_{\max(i)} e^{-\frac{\left(v-v_{\max(i)}\right)^2}{2\sigma_{(i)}^2}} = \sum_{i=0}^{n} E_{\max(i)} e^{-100\frac{\left(\frac{1}{\lambda}-\frac{1}{\lambda_{\max(i)}}\right)^2}{2\sigma_{(i)}^2}} \quad (5)$$

The Gaussian band of the absorptivity is symmetric if recorded linearly in energy such as the frequency ν and the wavenumber $\tilde{\nu}$, respectively; see Figure 2, top. It becomes asymmetric for a linear scale in wavelengths λ with a steeper edge to short and a less steep edge to long wavelengths; Figure 2, bottom. Gaussian curves (Figure 2, solid curves) are much faster, exponentially damped than Lorentzian curves (Figure 2, dotted curves) and cause for normal dispersion a spectral region where the index of refraction n is still comparably high, whereas the absorptivity κ is already damped to insignificantly small values; this is of special advantage for the generation of materials with high index of refraction for optical dispersing devices or light scattering. The latter is important for white pigment because strongly light scattering crystallites with micrometer dimensions (elastic light scattering) are required such as titanium dioxide (rutile) and zinc sulfide as well as organic pigments [11] such as the pteridines in wings of butterflies [12] or technical [13] organic white pigments. Their strong light absorption close to the visible region makes these substances also interesting as UV sun protectors [14].

The theoretical treatment of the interaction of light with matter with the resulting eq. (2) visualized in Figure 2 is experimentally verified with aqueous solutions of fluorescein (RN 2321-07-5, see below **2**) where the optical properties are reported in Figure 3. The absorption spectrum (solid curve) is exponentially damped at the bathochromic edge (highest energy) where a Gaussian analysis according to eq. (5) indicates several individual bands (bars). The composed spectrum on the basis of this analysis (dotted dashed curve) is nearly completely covered by the experimental spectrum and indicates the quality of the fit (actual to theoretical comparison).

$$n = a \cdot \frac{v_o^2 - v^2}{(v_o^2 - v^2) + \gamma^2 v^2} + n_o = a \cdot \frac{1/\lambda_o^2 - 1/\lambda^2}{(1/\lambda_o^2 - 1/\lambda^2) + \gamma^2/\lambda^2} + n_o = a \cdot \frac{\lambda^2 - \lambda_o^2}{(\lambda^2 - \lambda_o^2) + \gamma^2 \lambda_o^2} + n_o \quad (6)$$

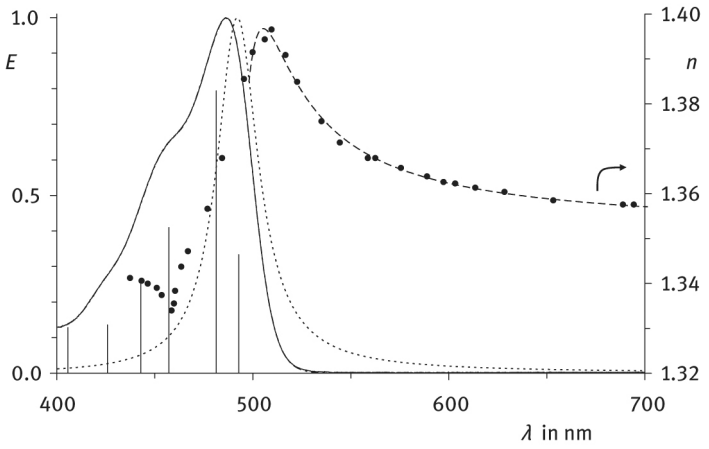

Figure 3: Normalized absorption spectrum of Fluorescein (RN 2321-07-5) in aqueous solution (solid curve, left scale E) and Gaussian analysis for the individual absorption bands (λ_{max} = 492.8 nm, 2 σ^2 = 0.239 kK, E_{max} = 0.333 and λ_{max} = 481.3 nm, 2 σ^2 = 0.669 kK, E_{max} = 0.794 for the most bathochromic) with bars for the positions and intensities and the simulated spectrum on the basis of the analysis: Dashed dotted curve, nearly completely covered by the experimental spectrum. Index of refraction n with the right scale; points: Experimental data according to ref [15].; dashed curve: Least square fit according to eq. (4), left (ν_o = 23.53 kK corresponds to 492 nm, γ = 2.076, a = 2.089, n_o = 1.347). Dotted curve: Calculated κ values (correspond to E) by means of the data obtained from n.

The experimental index of refraction [15] is shown in Figure 3 by points. The bathochromic branch above 500 nm is fitted to the parameters a, λ_o, γ and n_o of eq. (6) where n_o is the index of refraction of the medium and the other term the real component of eq. (4). n_o (1.347) is close to the applied medium water (1.332). The anomalous dispersion below 500 nm is complicated because of the overlay of several bands and was not further considered. The best fit for more than 500 nm is indicated by the dashed curve where the limited precision of the measurements have to be taken into account (some aggregation of the dye may have further influenced the measurements). The normal dispersion can be clearly seen where a monotonous decrease of the index of refraction is found above 510 nm. The obtained parameters λ_o and γ allow the construction of a hypothetical

absorption band (dotted curve), if there would be a homogeneous macroscopic light absorption. This band is close to the first Gaussian band, however, tails much more into the bathochromic region than the experimental exponentially damped and is a further indicator for the individually stochastically operating molecular resonators. This is of importance for highly refractive materials with low residual light absorption.

3 Molecular resonators

Inelastic light scattering requires the uptake of light energy and thus, appropriate energetic eigenvalues of the involved matter. A partial absorption of light energy proceeds in Raman spectroscopy with some energy transfer to molecular vibrations where the residual spectrum is characteristic for the chemical structure. A complete absorption of light energy causes electronic excitation where a characteristic impression of color is generated for absorption in the visible.

A typical energetic sequence of discrete electronic energetic eigenvalues is schematically indicated in Figure 4, left. These can be filled with electrons according to the aufbau principle where each distinguishable level can be filled with maximal two electrons with antiparallel spins according to Hund's rule and the Pauli principle, respectively. There is an even number of electrons for the very most organic compounds and one energetically upmost occupied orbital (HOMO). As a consequence, all electron spins are paired and such molecules form a singlet state named S_o. The index 0 indicates the electronic ground state; see Figure 4, left. Accordingly, the corresponding first electronically exited state is S_1 and so on; see Figure 4, left. The restrictions by the Pauli principle are still no more given for the S_1 and higher states because different orbitals are involved in the energetic upmost electrons. As a consequence, a second electronically excited state can be realized with two parallel spins in the two upmost orbitals forming a triplet state because the added electron spins; accordingly, this is named the T_1 state. The antiparallel arranging of spin is unfavorable where the required energy of this paring depends on the chemical structure. As a consequence, the T_1 state is generally located more or less below the S_1 state. The electronic excitation is interlinked with vibronic eigenvalues and with molecular rotation in the gas phase with some line broadening by the Doppler effect. As a consequence, a comparably complicated system results. Thus, the electronic energies of individual occupied orbitals were summarized for simplification in Jablonski's diagram in Figure 4, right, resulting in the basic electronic levels S_o, S_1 and so on. The vibronic and rotational levels are indicated by larger and smaller lines in Figure 4, right. Rotation is hindered in the condensed phase resulting in libration vibrations. The latter are not as well defined as the energetic levels of rotation in the gas phase because of fluctuating interactions with nearest neighbors and coupling with translation motions. As a consequence, a further line broadening and a quasicontinuum of energetic levels results for the latter in the spectral region of rotation spectroscopy. Finally, the comparably strong coupling of vibration and libration vibrations with the levels of electronic excitation further increases the complexity; however, density maxima still remain around the initial levels of vibration. As a consequence, there is a densely packed ladder of energetic levels for vibration and libration vibrations where S_o ground state forms the lower energetic limit. A similar sequence of energetic levels will be found for the S_1 state, preferently for complex molecules, because one chemical bond only is half loosen in S_1 compared with S_o and this concerns comparably weak π-bonds for most dyes molecules (see below). Such sequences of energetic levels are also found for S_2 and higher levels and for T_1 and higher triplet states where density maxima and minima are less pronounced for the latter. Light absorption proceeds between energetic levels of these ladders as a fast process in about 10^{-15} s where a movement of the heavy nuclei is of minor importance (however, see ref [16, 17].) and the molecular geometry remains essentially unaltered ("vertical" processes); a subsequent relaxation into a local energetic minimum may proceed.

$$\frac{n_+}{n_-} = \frac{g_+}{g_-} \cdot e^{-\frac{\Delta E}{RT}} \tag{7}$$

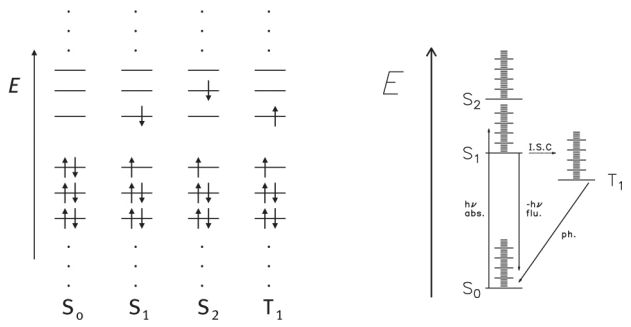

Figure 4: Left: Term scheme of the electronic excitation of dyes. Right: Jablonski's diagram: *hν* abs. electronic excitation with light absorption, *hν* flu. fluorescence, ph. phosphorescence.

Essentially, the energetic ground state of S_o is populated at room temperature; this can be seen by the application of Boltzmann's equation (7) where generally the population of an upper energetic level n_+ over the lower level n_- is given by the ratio of the statistical weights g_+ and g_- (unity for complex non-symmetric molecules) multiplied with the exponential ratio of the energetic difference ΔE of the involved levels and the thermal energy RT. Thus, the thermal energy at room temperature (2.4 kJ·mol^{-1} at 20 °C) is not sufficient for a significant population of upper vibronic levels (about 18 kJ·mol^{-1} at 1500 cm^{-1}). As a consequence, the S_o ground state can be taken as the initial state for electronic excitation at room temperature. The molecular multiplicity is not affected by the process of light absorption proceeding into electronically excited S states because of spin conservation. An excitation into T states would require a simultaneous inversion of an electron spin, is indicated as a spin forbidden process and thus, proceeds with a very low probability; some paramagnetic substances, for example molecular oxygen, may favor such transitions (compare the very weakly brownish color of highly pure air-saturated benzene). The light-induced electronic transition from the S_o ground state may proceeds not only into the S_1 ground state (0-0-transition), but also into vibronically excited states; sharp individual electronic transitions were found in the gas phase (with the mentioned some line broadening by the Doppler effect), whereas strong line-broadening proceeds in the condensed phase with increasing molecular interactions where there are still maxima of transition probability close to the initial molecular vibronic levels. As a consequence, the ladder of states is projected to the UV/Vis absorption spectrum [18] where a bathochromic limit is found and a more or less structured continuation to shorter wavelengths (compare that the wavelength is the inverse to the energy of absorption; see eq. (1) above). The efficiency of molecular light absorption is characterized by the wavelength-dependent molar absorptivity interrelated with the oscillator strengths; the latter is important for quantum chemical calculations. The absorption spectrum linearly recorded in energy such as the frequency or wave number can be composed by a sum of individual Gaussian bands according to eq. (5) where the branch at longest wavelengths is exponentially damped [19] with the square of wavenumber; accordingly, the damping proceeds with the inverse square for the wavelength. Very weak absorptions at longer wavelengths sometimes observed with practical samples proved to be caused by low residual contents of by-products and could be removed by means of progressed chemical purification.

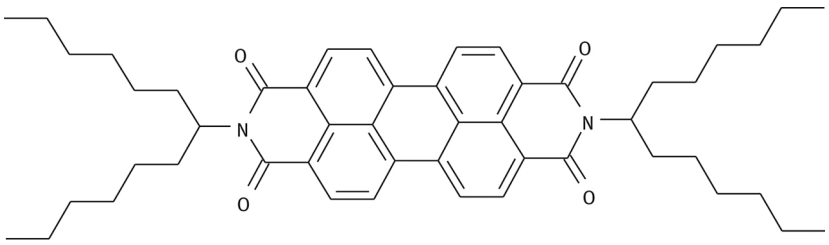

S-13 (**1**; CAS registry number RN 110590-84-6)

S-13 (**1**; CAS registry number RN 110590-84-6)

Optical excitation with even higher energy at shorter wavelengths allows reaching higher electronically states such as the S_2 and S_3 state. As a consequence, the structured absorption continues to shorter wavelengths where there may be intense absorption bands in the UV.

4 Basics of fluorescence

The vibronically excited S_1 state looses the vibronic excitation in a very short time in the order of 0.1 ps (10^{-13} s) to become thermal energy. The strong coupling of the vibronic modes causes the equilibration of the vibronic energy within one or a few periods so that the S_1 ground state is reached exhibiting a longer lifetime of some nanoseconds (10^{-9} s). A similarly fast relaxation of higher electronically excited states to the S_1 ground state is observed for nearly all organic molecules (azulene is a prominent exception [20]) so that this state is generally the origin for the further light-induced processes. A simple interconversion (I.C.) from the S_1 state to a highly vibronically excited S_o state may proceed and is followed by a fast relaxation to the ground state and the dissipation of the energy, finally to produce heat. This describes the function of the majority of textile dyes and technical pigments where the selective light absorption causes an impression of color. Some dyes are able to re-emit the absorbed energy with a process named fluorescence [21]. Starting with the S_1 ground state the ladder of energetic levels of the S_o state will be reached where the maximal energy will be obtained by the transitions between the vibronic ground states. As a consequence, there is a limit of the spectrum of light emission at high energy and short wavelengths, respectively (hypsochromic limit). Moreover, the energetic ladder of the S_o state is very similar to the ladder of the S_1 state in most cases for complex molecules because only one chemical bond is half loosened and this influences unimportantly the vibronic force constants (see above). As a consequence, the wavelengths-dependence of the fluorescence spectrum looks about like mirror-type of the absorption spectrum (known as the Stokes' mirror type spectra); this is demonstrated with the typically structured spectrum in Figure 5 of the for the perylene derivative [22] S-13 (dye **1**).

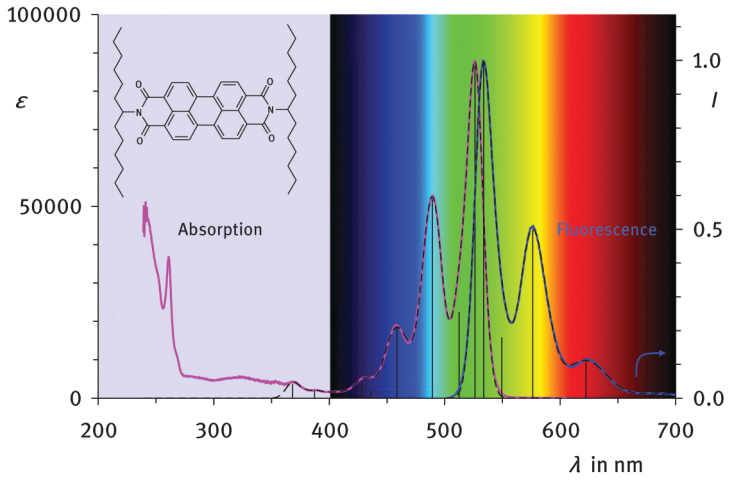

Figure 5: Absorption (left magenta curve) and fluorescence (right blue curve) spectra of the perylene dye **1** (S-13) in chloroform. Bars: Positions and intensities of the calculated individual Gaussian vibronic bands. Dotted curves: Simulated spectra on the basis of the Gaussian analysis (mainly covered by the experimental spectra). The fluorescence quantum yield of **1** is close to unity.

The process of fluorescence seems to be simply the reverse of the absorption at the first glance (Stokes' mirror image of absorption and fluorescence spectra). However, there are important differences. Firstly, the intensities of the sequence of vibronic bands of fluorescence (Figure 5, right spectrum with a blue curve) obviously become faster damped with increasing wavelengths than in the absorption spectrum to shorter wavelength (Figure 5, left spectrum with a magenta curve). This can be attributed to the mismatch of the wavelength of radiation with the dimension of the antenna. For example, the mean wavelengths of absorption and emission of **1** in Figure 4 is about 500 nm where suitable dimensions of antennae are $\lambda/2$ and thus, 250 nm (the index of refraction has to be considered for fine tuning). However, the chromophore of **1** extends over no more than 1 nm; this is the effective length between the two nitrogen atoms as the termini of the conjugated system. Thus, the mismatch is important for absorption and becomes slightly minor for the higher vibronic bands at shorter wavelengths. However, the mismatch becomes worse for higher vibronic bands in fluorescence because of longer wavelengths. This effect is described by Rüdenberg's formula [23] for classical treatment of electromagnetic radiation with radio antennae and in the same manner with the equivalent Ross' equation [24] obtained by quantum mechanical treatment. The 0–0 transition should be identical in absorption and fluorescence; however, one generally finds the fluorescence maximum slightly or even more pronounced situated at longer wavelengths known as the Stokes' shift. Relaxation processes of the excited state into a new geometry are therefore responsible because the optical excitation changes slightly the force constants of chemical bonds; this shift is small in the spectra of firm, rigid compounds such as for **1** in Figure 4. Larger changes in molecular geometry by relaxation may

cause appreciable Stokes' shifts. Finally, the ratio of emitted light quanta over the number of absorbed is known as the fluorescence quantum yield Φ and can extend from zero to unity. There are few examples of dyes with fluorescence quantum yields larger than 0.7.

5 Optical excitation of fluorescent molecular structures

A light wave passing a diluted solution of well-separated independently operating dye molecules is not continuously damped such as radio waves from absorbing materials, but induces individual molecular electronic transitions. These individual processes are not determined; however, the transition probability remains constant. The very large number of dye molecules in practical samples averages the individual processes to a constant damping of the wave. The light-absorbing [25] is well described by Lambert Beer's law of eq. (8) where I_o is the intensity of the incoming monochromatic light and I the intensity after the absorbing light pass where the decadic logarithm (lg) is applied for historic convenience to obtain the absorptivity E.

$$lg\frac{I_o}{I} = E = \varepsilon \cdot c \cdot d \tag{8}$$

The dimensionless E is proportional to the concentration c and the path length d where the factor ε is known as the coefficient of extinction (the coefficient of absorption A may be more characteristic for the chromophore because ε becomes diminished for strongly fluorescent samples; however, this effect is very small for standard spectrometers because of the small efficient solid angle of the applied nearly parallel light beam). For convenience, d is measured in cm and c in mol/L and thus $L{\cdot}mol^{-1}{\cdot}cm^{-1}$ is the dimension of ε as the decadic molar coefficient of extinction. The wavelengths-dependent ε can range from small value to more the 100,000 in maxima of strongly light-absorbing chromophores. Thus, even weakly light-absorbing materials would efficiently absorb light if the path length is long enough; for example, even obviously clear, transparent natural water weakly absorbs light so that the grounds of lakes become dark for more than 20 m depths. The coefficient ε depends from the wavelength λ and is generally recorded as UV/Vis spectra. Maxima of ε are commonly applied for the characterization of dyes where the integral of the absorption band is a more appropriate measure for the oscillator strengths of the chromophore because it can be interrelated with quantum chemical methods; however, the determination is more difficult because of partial overlap with bands of higher excitation. On the other hand, the half widths of most absorption bands are similar. Thus, the absorptivity at the maximum is well suitable for a rough, global characterization of chromophores. Lambert-Beer's law is frequently applied for the optical determination (E) of chemical concentrations c with comparably high precision and comparably low experimental effort; however, one has to take care (i) to allow to operate the spectrometer in the appropriate range (about $0.3 < E < 1.0$), (ii) that there is no interaction of dye molecules such as aggregation (sufficient dilution), and (iii) to apply monochromatic radiation because eq. (8) is valid only for one wavelength, but not for a spectral range. Such errors become minimal for measurement in the maxima because of minimal change of ε in a small spectral rage around the maxima.

6 Fluorescence

The application of Jablonski's diagram (Figure 4, right) may transmit the impression that the absorption of a light pulse would cause an echo of fluorescence similar to the RADAR for radio waves, possibly with some delay caused by molecular processes; *however, this is definitively not the case*. The macroscopic electromagnetic light wave passes many individual chromophore with barriers for electronic excitation with constant transition probabilities where the individual processes are not predictable. In a very rough calculation a concentration $3.01{\cdot}10^{-6}$ mol/L of a strongly light-absorbing dye with ε = 100 000 is required for the absorption of 50% of the incoming light (50% transition probability) within 1 cm path of an optical standard cuvette. In a cylinder with the diameter of the wavelength of about 500 nm and 1 cm path about 4 million dye molecules are involved until a 50% transition probability for absorption is reached. Here, one can see that absorption will proceed if only the optical path is long enough.

The conditions for fluorescence are absolutely different because the energy of electronic excitation is localized to an individual molecular structure where a barrier to the evolution of a free electromagnetic wave has to be passed. This proceeds by tunneling [26] this barrier such as is also known for the radioactive decay. Indeed the fluorescence decay generally proceeds exponentially according to the same first-order-law with the time constant τ of some nanoseconds where the probability of the process is independent from the already

elapsed time (compare the well-known radioactive decay; multi exponential decays are observed if more than one process is involved). The fluorescence of optically excited molecules has to compete with other processes of deactivation such as the internal conversion I.C. Competing processes for deactivation lower the fluorescence quantum yield Φ and the experimental time constant where the natural time constant τ_0 can be calculated by means of eq. (9).

$$\tau = \Phi\tau_0 \tag{9}$$

The two time constants τ and τ_0 become essentially equal for highly fluorescent chromophores (Φ ≈ 1) such as **1** where 4 ns were observed in chloroform. The time constant τ_0 depends on the transition probability from the S_1 ground state to the S_o levels and is roughly inversely proportional to the molar absorptivity. This is quantitatively indicated by the Strickler–Berg-Equation (10) [27] initially established by Förster [28] where the inverse of the fluorescence lifetime τ_0 is equal to Einstein's transition probability $A_{u\to l}$ from the upper (u) to the lower (l) state. This is equal an expression of some constants such as Avogadro's number N_A, ln (10) for the adaption of the decadic absorptivity ε to SI units, the velocity of light c, the wavenumber $\tilde{\nu}_{u\to l}$ for the transition from u to l, n the index of refraction, g_l and g_u the statistical weight and the integral over the absorption band linear in wavenumber.

$$\frac{1}{\tau_0} = A_{u\to l} = 1000\frac{8\pi\ln(10)c\tilde{\nu}_{u\to l}^2 n^2}{N_A}\frac{g_l}{g_u}\int \varepsilon d\tilde{\nu} \tag{10}$$

Equation (10) can be applied in many cases, preferment for series of similar compounds, however, there are exceptions. Short fluorescent lifetimes τ_0 are expected for strongly light-absorbing dyes with comparably broad absorption bands such as **1** where 4 ns were observed; however, the weaker light absorbing diketoterthiophenes unexpectedly exhibit an appreciably shorter fluorescence lifetime [29] of only 0.4 ns.

Moreover, the fluorescence lifetime τ_0 according to eq. (10) is estimated to be a molecular property and thus, independent from the chemical concentration of highly diluted solutions of isolated molecules. In contrast to the theory, a fluorescence lifetime of 5 ns is found for an already diluted $2{\cdot}10^{-5}$ molar solution where the lifetime is diminished to 3.8 ns by further dilution to $1{\cdot}10^{-7}$ molar [30]; see Figure 6. This unexpected result may be interpreted in terms of evanescent waves [31] and the tunnelling where the evanescent waves were reflected by the other identical not electronically excited chromophores thus, retarding the tunnelling. This new far-reaching effect over more than 100 nm basically allows molecular addressing by macroscopic structures. Finally, fluorescence lifetime and the influencing by the molecular surrounding are obtaining increasing importance for imaging [32] in biology and medicine (FLIM) because of detailed microscopic information.

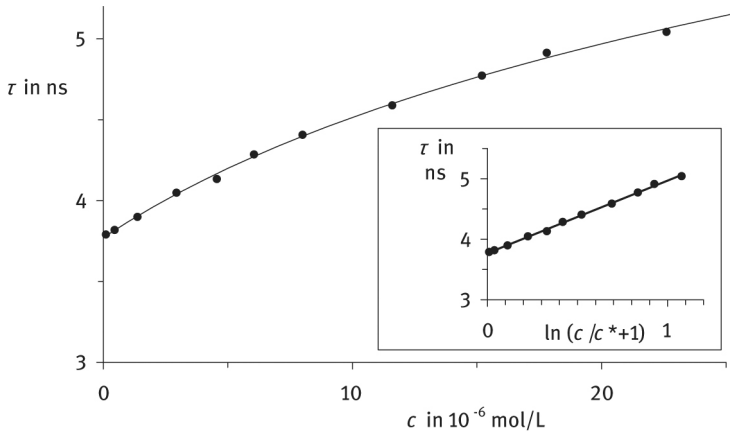

Figure 6: The fluorescence lifetime τ of **1** in chloroform as a function of concentration c in mol/L. Inset: Linearization of the curved plot with $c^* = 1.17{\cdot}10^{-6}$ mol/L.

7 Prerequisites for strong fluorescence

To obtain highly fluorescent materials, natural light emission characterized by the natural lifetime τ_0 has to compete with other processes of deactivation such as internal conversion (I.C.) to highly vibronically excited electronic ground states. Such competing processes are efficient for the majority of organic compounds, whereas

low molar absorptivities diminish the transition probability for spontaneous light emission; as a consequence, organic materials, preferentially dyes, are generally non fluorescent ($\Phi < 0.001$) and comparably few basic chemical structure with high fluorescence quantum yields are known. Special chemical and photo physical requirements can favor fluorescence such as high molar absorptivities increasing the transition probabilities, and rigid chemical structures for lowering possibilities for radiationless decays by means of internal conversion according to the loose bolt mechanism defined by Lewis and Calvin [33]. There are only few strongly fluorescent materials. Fluorescein [34] (**2**, RN 2321-07-5), developed by Adolf von Baeyer, is one of the most prominent examples, is intensely green fluorescent in aqueous solution; uranine is a further name for **2** and its di-sodium salt (RN 518-47-8), respectively, because the yellowish color in absorption of aqueous solutions and the yellowish green fluorescence resemble the color of solutions of uranylium compounds and uranium glasses, respectively, the most prominent fluorescent materials at the time of the discovery of **2**.

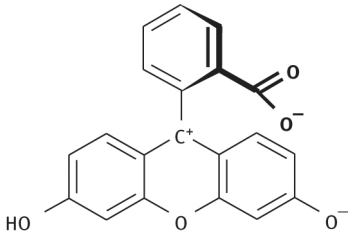

2

Basic structural prerequisites for strong fluorescence can be rationalized with **2**. The arrangement of two donor-substituted (–OH and –O⁻) phenyl groups with a formal carbenium ion in between as an acceptor allows a high molar absorptivity and a comparably bathochromic absorption in the middle of the visible region according to the principle of König and Ismialski [35]. The linking of the two phenyl units by means of an oxygen atom forming the rigid heterocycle xanthene restricts the intramolecular mobility of the chromophore; degrees of freedom coupling to the system of electronic excitation are most important concerning fluorescence quenching, whereas peripheral alkyl groups such as rotatable methyl groups are of minor influence. Further restriction of internal rotation in **2** causes the carboxylate group because of steric interactions with the neighboring hydrogen atoms in the *peri*-positiones of the xanthene. The limitation to light chemical elements in **2** (carbon, hydrogen and oxygen) is favorable for intense fluorescence because heavy elements favor the inter system crossing (I.S.C.) to the triplet as a competing and deactivating process: A molecule of light elements form essentially isolated spin and orbital systems with weak coupling, whereas heavy elements support spin orbital coupling (Russell-Sounders coupling) [36, 37] and favor I.S.C. Moreover, the orthogonal arrangement of the carboxyphenyl group disfavors aggregation as a possible further source of fluorescence quenching. Finally, the negative charge lowers the tendency of aggregation in the aqueous phase by electrostatic repulsion. As a consequence, a fluorescence quantum yield of more than 90% is observed aqueous solutions of **2**.

The UV/Vis spectra of **2** are recorded in Figure 7 with the left magenta curve for the light absorption. This mainly extends to the spectral range of blue light and generates a yellow impression because of the complementary color. The emitted green fluorescent light (right blue curve) extends around the sensitivity maximum of the human eye and generates an impressive color effect with a brilliant shade because of the small half widths of the emission spectrum.

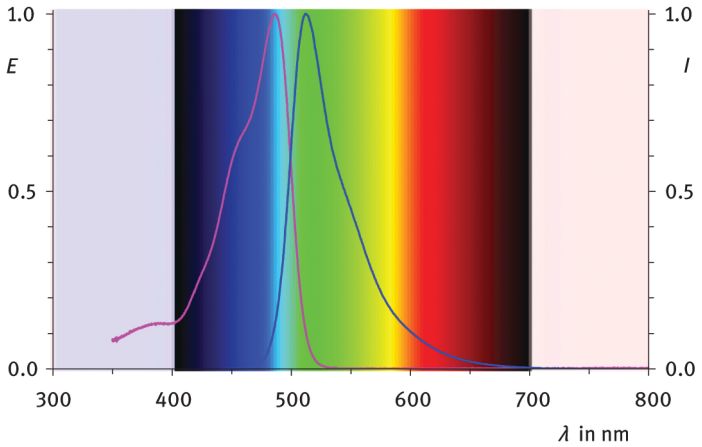

Figure 7: Absorption (left, magenta curve, left scale) and fluorescence (right, blue curve, right scale) of Fluorescein (**2**, RN 2321-07-5) in water.

The photostability of **2** is comparably low. The donor groups –OH and $–O^-$ favor oxidative degradation. Their exchange to electrically neutral nitrogen-based donor groups increase the photostability appreciably where alkylation to form tertiary amines prevent degradation processes initiated by deprotonation. The donor effect of a dialkylamino group concerning chromophores is roughly about the same effect of a deprotonated phenolic oxygen atom. As a consequence, the replacement of the donor groups in **2** by means of diethylamino groups in **3** (Rhodamine B as the chloride) causes an appreciable bathochromic shift in absorption and fluorescence and a significant improvement of the photostability; see Figure 8. This class of compounds is known as the rhodamine dyes where **3** is one of the most prominent.

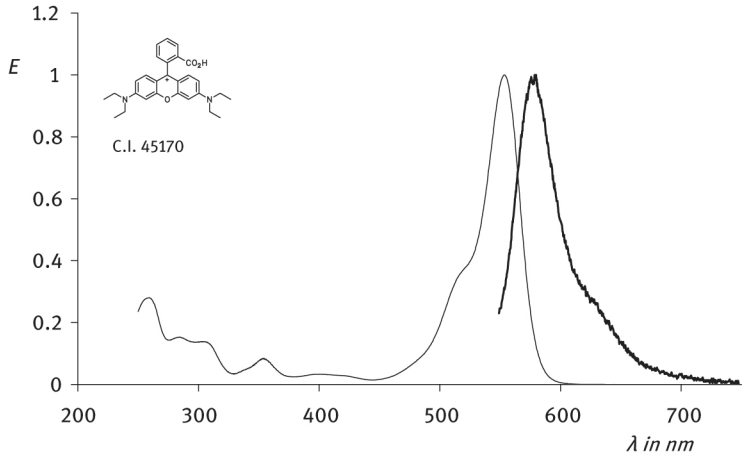

Figure 8: UV/Vis spectra of Rhodamine B chloride (**3**, RN 81-88-9, C.I. 45,170) in water. Left: Absorption spectrum, right: Fluorescence spectrum.

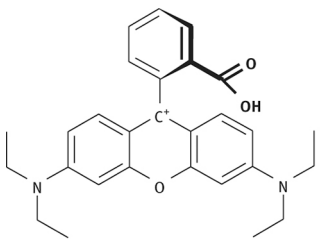

3

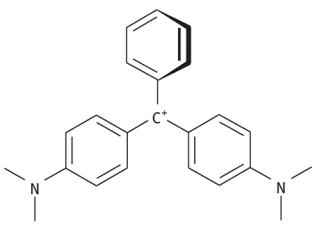

4

The effect of intra molecular mobility on the fluorescence can be clearly seen with the comparison of the strongly fluorescent Rhodamine B (**3**) with the non-fluorescent Malachite Green (**4**, RN 569-64-2). The fluorescence de-

activation of the latter can be attributed to the freedom of rotation around the single bonds of the dimethylaminophenyl groups to the formal carbenium ion. These degrees of freedom are significant concerning the electronic excitation, whereas freedoms of rotation in the alkyl sidechains such as with **3** are of unimportant influence concerning the chromophoric system. The photostability of **3** is appreciably improved compared with **2** because of the more suitable donor groups; however the photostability is only just acceptable for many applications. Some inter system crossing (I.S.C.) to the triplet state and subsequent sensitizing of the triplet oxygen to form singlet oxygen is an important path for the photochemical degradation of dyes because the latter exhibits reactions of an electron depleted reactive olefin such as Diels–Alder reactions and degrades chromophores. The I.S.C. becomes even more pronounced by the introduction of heavy elements such as the four bromine atoms in Eosin (**5**, RN 17372-87-1). The strong electron withdrawing effect in **5** gently lowers the tendency for oxidation and increases the acidity of both phenolic groups so that an appreciable bathochromic shift in the absorption is reached by two strong donor groups and a full deprotonation proceeds in aqueous solution; as a consequence, Eosin (**5**) is applied as red ink where the fluorescence is much weaker than in **2**. The replacement of the bromine atoms in **5** by the even heavier iodine atoms (Erythrosin, RN 568-63-8) favors further the I.S.C. Finally, a chlorination for diminishing the tendency of oxidative degradation makes the similar Rose Bengale (**6**, RN 632-69-9) useful as a singlet oxygen sensitizer in preparative chemistry ($\Phi_{\text{I.S.C.}} > 0.9$ [38] where $\Phi_{\text{flu.}} \approx 0.1$ remained). Chlorination is generally frequently applied for the stabilization of dyes.

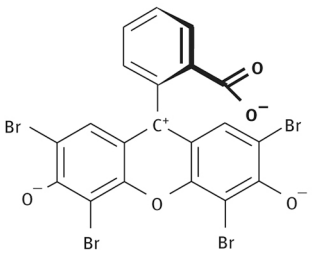

5

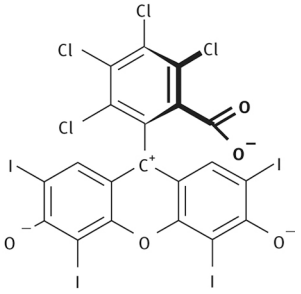

6

The limited photostability of xanthene derivatives prompted the development of many other fluorescent chromophores [39, 40] with high fluorescent quantum yields [41, 42]. Examples [43] are the coumarines **7**, where the disubstituted amino group as a donor induces bathochromic spectral shifts of fluorescence until the visible. The fluorescent natural product Aesculine (see above) is a similar coumarine, however less stable than **7** because of OH groups as a donors instead of the amino group in **7**. Various aryl and heteroaryl substituents may be applied in **7** forming a formal stilben substructure. Indeed, stilbenes substituted with amino groups such as **8** where the sulphonate groups are introduced for water solubility are applied as fluorescent whitening agents. Finally naphthalimides such as **9** are highly photo stable. **9** absorbs mainly in the UV and exhibits a blue fluorescence. The exchange of the methoxy group as a weak donor by an aminogroup as a stronger one causes a bathochromic shift both in absorption and fluorescence. Numerous further fluorescent materials are known with many applications such as the fluorescent natural product quinine (RN 130-95-0).

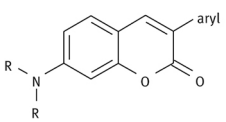

7

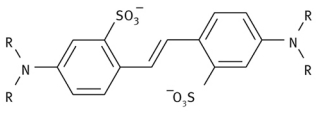

8

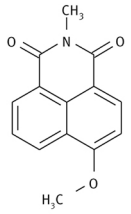

9

Unusually high photostabilities and fluorescence quantum yields exhibit the *peri*-arylenes **10** [5] known for $n = 1$ to $n = 4$ and $n = 6$. Moreover, there is only one electronic transition in the visible parallel to the *N*-*N*-connection

line making the analyses of interactions of chromophores clear. As a consequence, here we concentrate further discussions mainly to **10**.

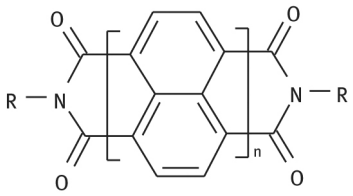

10

The naphthalenecarboximides (**10**, $n = 1$) absorb in the UV [44] and may be applied as white pigment [45] or for sun protection [46]; see Figure 9. The fluorescence is comparably weak because the S_1 state is close to a further, non-fluorescent state [47] and looses energy of excitation by their interaction. The perylenebiscarboximides (**10**, $n = 2$ where **1** is a special derivative because of the solubilizing *sec*-alkyl groups) as the next higher homologues generally exhibit a very low solubility and are applied as photostable pigments [48] such as the methyl derivative (R=CH_3) C.I. Pigment Red 179 (RN 5521-31-3). The low solubility of the perylenebiscarboximides [49] and their higher homologous could be resolved by solubility increasing groups R such as 2,5-di-*tert*-butylphenyl group (RN 83054-80-2) [50], 2,6-di–*iso*-propylphenyl group [51] or the even more efficient long-chain secondary alkyl groups [52] such as the here reported 7-tridecyl group [53]. The latter is a good compromise between efficiency and peripheral ballast to the chromophore where the two identical long-chain hexyl groups prevent the introduction of stereogenic centers to keep the purification of the dyes simple and efficient. The soluble perylene dyes are highly fluorescent where quantum yields close to unity were observed so that **1** may be used [54] for the calibration of fluorescence spectrometers because of the extraordinarily high photostability [55] as a prerequisite for long-term stable signals.

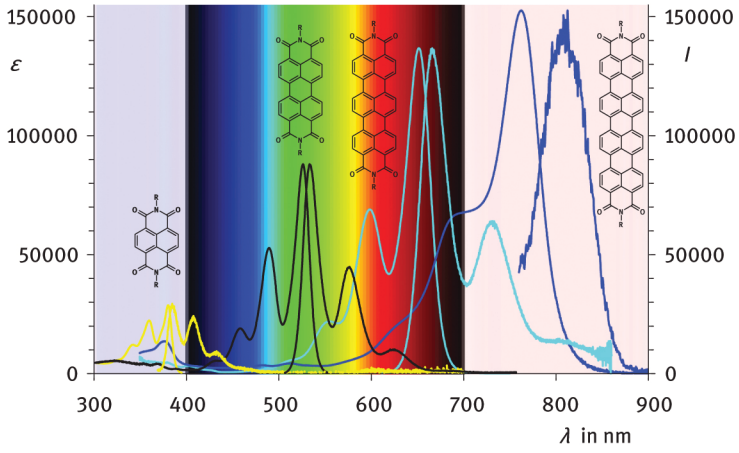

Figure 9: UV/Vis absorption (left curves and left scale, in L·mol·cm^{-1}) and to the absorption normalized fluorescence spectra (right curves and right scale) of *peri*-arylenes **10** in chloroform; R means the long-chain secondary alkyl substituent 7-tridecyl for solubilisation, and 1,5-dichloro-3-pentyl for $n = 1$. From left to right naphthalenebiscarboximides (**10**, $n = 1$, yellow curves), perylenebiscarboximides (**10**, $n = 2$, black curves), terrylenebiscarboximides (**10**, $n = 3$, turquoise curves), and quaterrylenebiscarboximides (**10**, $n = 4$, blue curves with limited accuracy in the bathochromic branch of fluorescence).

The terrylenecarboximide (**10**, $n = 3$, RN 1403692-73-8) [56] is the next higher homologous and forms strongly red fluorescent blue solutions where a quantum yield close to unity allows the application for the calibration in the more bathochromic spectral region. Finally, the quaterrylenecarboximide (**10**, $n = 4$, RN 168101-28-8 P) [57, 58] absorbs partially in the NIR. The fluorescence spectrum extends in the NIR above 800 nm; fluorescence quantum yields were not yet determined. The sexterrylenecarboximide (**10**, $n = 6$, RN 168101-28-8 P) [59] fully absorbs in the NIR with a maximum at 945 nm; it is still not investigated if there is fluorescence at very long wavelengths.

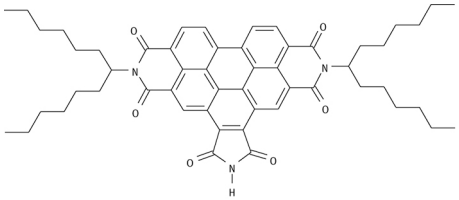

11

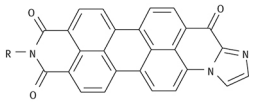

12

Derivatives of (**10**, $n = 2$) such as **1** are mostly applied for fluorescence applications because absorption and fluorescence are in the middle of the visible region and the perylenetetracarboxylicbisanhydride (RN 128-69-8, C.I. Pigment Red 224) as the starting material for syntheses is a technical mass product [60]. The position of the absorption and fluorescence spectra can be fine-tuned by means of an extension of the core and by alterations of the peripheral carboximide structure. A core substitution with donor groups cause bathochromic shifts [61–63], whereas hypsochromic shifts can be obtained by the lateral extension of the core such as in **11** [64]. The introduction of an imidazole ring into the periphery in **12** shifts the absorption and fluorescence spectra [65] exactly into spectral region of for spectroscopic investigations interesting hydrocarbon terrylene; however, **12** is appreciably more chemically and photo chemically stable than the labile terrylene.

8 Dynamic processes

The Stokes' shift of **1** and similar fluorescent dyes is comparably small causing an appreciable overlap between the absorption and fluorescence spectra. A larger spectral separation would bring about an appreciable advantage for some applications of fluorescent dyes such as for fluorescent solar collectors [66] and dye lasers [67] because of diminished re-absorption of the fluorescent light.

The Stokes' shift can be increased by means of dynamic processes M and M' in the timespan between the optical excitation of about 10^{-15} s with subsequent thermal relaxation to the S_1 ground state of about 10^{-13} s and the lifetime of the exited S_1 state of some nanoseconds; see Figure 10. The movement of electrons is in the timescale of the electronic excitation and does not cause effects of relaxation. However, the movement and relaxation of the heavier nuclei proceeds more slowly, but is still fast enough to be finished within the lifetime of the excited state. Fast chemical processes M are suitable to reach the S_1' state with some energy loss before deactivation; the remaining energy of excitation becomes diminished and thus, the fluorescence is bathochromically shifted [66]. Finally the energetic position of the S_o' state must be above the S_o state to reach the latter by M' in a cyclic process to avoid a photochemical consumption of the fluorescent dye. The stronger the molecular interactions for M and M' are the larger is the effect, but the more are the molecules stressed such as with excimer formation and this is frequently unfavorable for the photo stability. As consequence, one has to find compromises.

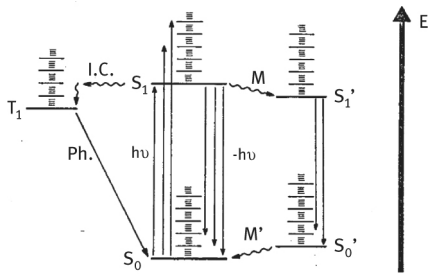

Figure 10: Jablonski-diagram for dynamic processes [66]. *hν*: Light absorption and *-hν*. Fluorescence, M and M': Relaxation processes.

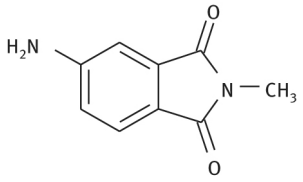

13

Solvent relaxation is a very gentile influencing where dye **13** [68, 69] is a strongly fluorescent suitable candidate for studies because the S_o state is only weakly polar with a small dipole moment, whereas the S_1 state exhibits a large dipole moment because of charge shift from the amino to the carbonyl group; as a consequence, the S_o ground state is only weakly solvated in polar media and this solvent shell is conserved in the S_1 state after electronic excitation; however, the geometry of this shell is unfavorable because the induced large dipole moment. As a consequence, the S_1' state is reached by solvent relaxation. Bathochromically shifted fluorescence proceeds to the S_o' state with a low dipole moment and again an unfavorable solvent shell. Finally, the S_o state is reached back again by the relaxation M'. The spectral shift of the solvatochromism in fluorescence is so pronounced that dye **13** is suggested as an empirical fluorescent solvent polarity probe [70]; for more details see ref [71]. The required polar media for an increase of the Stokes' shift can be realized with polar solvents and is more difficult attainable with polymers where a copolymerization with a polar monomer was finally successful [72]. The limitations concerning the polarity of the mediums are not given for molecules that change their geometry as the optically induced relaxation. This was demonstrated with DPP fluorescent dyes [73] (initially named diketopyrrolopyrrole, presently pyrrolopyrroledione) according to Figure 11. The phenyl groups were twisted out of the chromophore plain by steric interactions of the substituents R and thus, electronically decoupled causing a hypsochromic shift in the absorption. The electronic excitation increases the double bond character of this bond and turns the phenyl groups against the sterical stress in plane if the size of R is appropriate and thus, couples the phenyl groups to the chromophore, induces a bathochromic shift of fluorescence and an increase of the Stokes' shift.

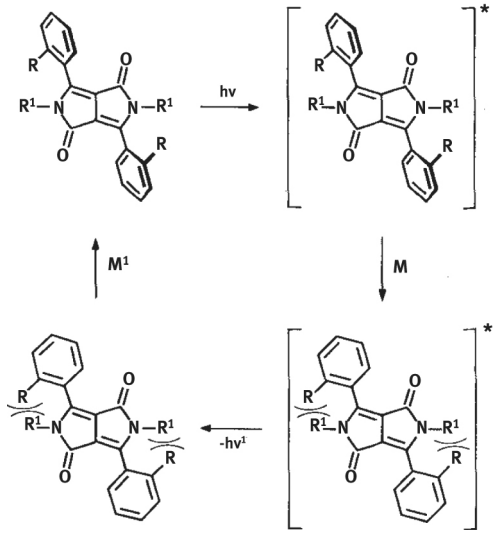

Figure 11: Dynamics in optically excited DPP fluorescent dyes by the mobility of a single bond; R = CH_3, relaxation M and M'.

The dynamic process around a single bond is combined with a solvatochromic solvent sensitivity in fluorescence in dye **14** (RN 2253747-09-8) [74]; Figure 12. Optical excitation induces a charge shift from the methoxynaphthalene in **14** to the perylene being a driving force M for a planarization (iPLICT mechanism [75]; incomplete planarized intra molecular charge transfer). The resulting increase of the dipole moment with the formation of the excited state allows a fine tuning of the energy by means of solvent effects and thus the color of fluorescence (*-hν'*). The concept of steering the optical properties of fluorescent dyes by means of molecular dynamics looks attractive; however, this means a balancing act because flexibility may cause fluorescence quenching by the loose bolt mechanism of Lewis and Calvin [76, 77], moreover, a strong tilting of the ground

state structure may end-up in a TICT mechanism [78] (twisted intra molecular charge transfer) with orthogonal substructures in the excited state; however, this seems to be less favorable for high fluorescence quantum yields [79].

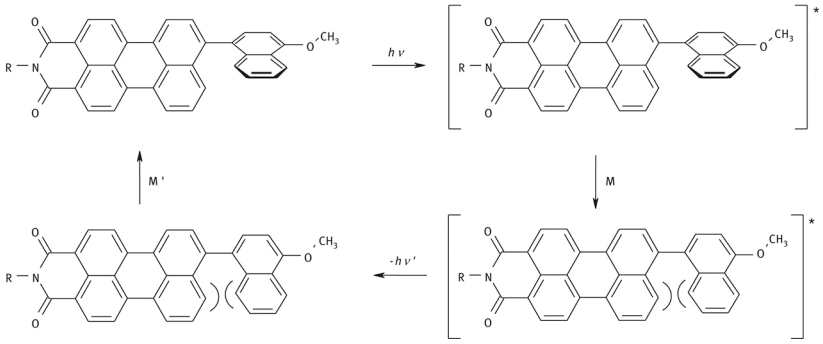

Figure 12: Dynamic process in perylene derivatives combined with a charge shift; dye **14**, R = 7-tridecyl. *hν*: Optical excitation inducing a charge shift from the methoxynaphthalene to the perylene. M and M': Relaxation. - *hν'*: Fluorescence.

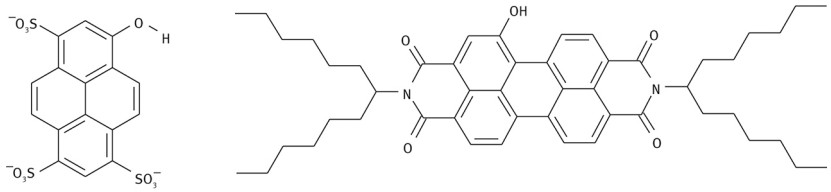

15 **16**

An even more pronounced influencing of electronically excited states is given by the breaking and forming chemical main valences. The breaking and forming of O–H and N–H bonds is fast enough to compete with the fluorescence decay. The OH group of the hydroxypyrenetrisulphonate **15** (RN 6358-69-6) [80] in neutral to slightly acidic aqueous solution is not dissociated. Light absorption with this weak donor group is found at comparably short wavelengths. Optical excitation shifts charge from the OH group into the aromatic nucleus and increases the acidity considerably. As a consequence, the OH group is deprotonated in a fast reaction forming the stronger donor group O^- and a considerable bathochromic shift in the fluorescence where a large Stoke' shift is observed with an intense green fluorescence and quantum yields close to unity by this ESPT (exited state proton transfer) mechanism [81]. The necessary aqueous medium with controlled acidity and the limited photostability of **15** mean restrictions for many applications. The ESPT mechanism can be also realized with the more stable perylene dyes such as **16** (RN 1018856-45-5) [82] even in more lipophilic media where amines may be applied as proton acceptors. The ESPT mechanism allows a separation between absorption and fluorescence spectra for **16**; see Figure 13.

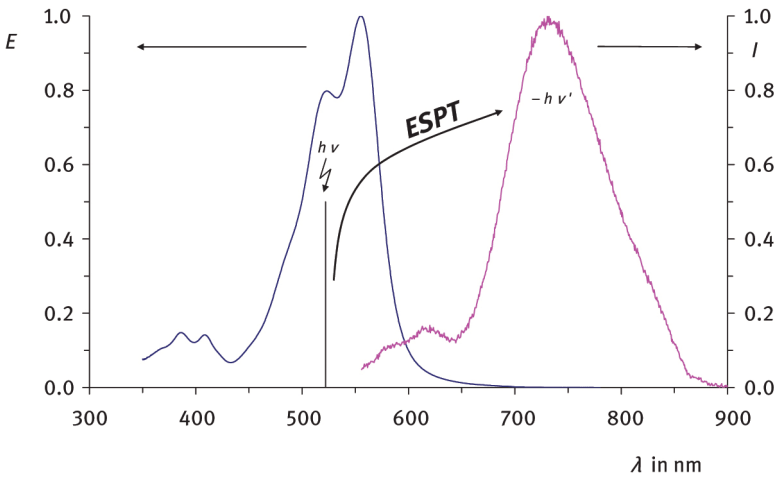

Figure 13: Absorption (left blue curve and left scale) and fluorescence spectrum (right magenta curve and right scale) of **16** in *N*,*N*-dimethylaniline as the proton acceptor. Bar: Wavelength for the optical excitation for fluorescence.

The ESPT mechanism requires a proton acceptor; This restriction can be avoided by means of an intramolecular proton acceptor where the light-induced process is named ESIPT (excited state intra molecular proton transfer). 5,5′-Dihydroxybipyridyl (RN 36145-03-6) [83, 84] exhibits suitable structure elements for such a process where a fluorescence quantum yield of only 0.31 is found [85]. An appreciably higher fluorescence quantum yield of about 50% is found for the dimethyl derivative **17** (RN 34237-07-5) [83, 86] where a baseline-separation of the absorption and fluorescence spectrum is obtained; see Figure 14. A double proton transfer is discussed as the reason for the spectral separation; however, details of the mechanism are still under consideration [85, 87–90].

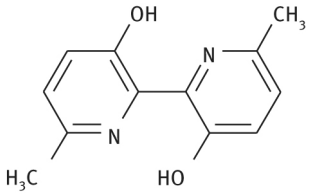

17

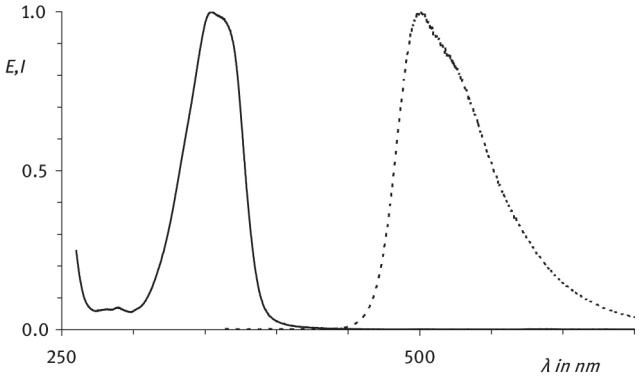

Figure 14: Absorption (solid curve left) and fluorescence spectra (dotted curve right) of the dimethylbipyridinediole **17** in chloroform.

Bipyridinedioles such as **17** exhibit chelating properties, for example for copper ions, forming non fluorescent complexes and can be applied for the analytical determinations of the ions with high sensitivity [91]; the large Stokes' shift avoiding re-absorption of the fluorescent light is of special advantage for such applications.

9 Energy transfer

Fluorescent materials conserve the energy of excitation for several nanoseconds and allow the processing of this energy by fast processes and thus useful for applications such as for molecular electronics. The energy transfer [92] from one chromophore to some other is an important process where the collection an transport of light energy in the photosynthesis reaction center [93] is the most prominent example. Essentially two mechanisms for the energy transfer are generally accepted (i) the Dexter mechanism [94] requiring a direct contact of orbitals and (ii) the Förster resonant energy transfer (FRET) [95] as a consequence of resonantly interacting dipoles of the hypsochromically absorbing energy donor and the more bathochromically absorbing and fluorescent acceptor. This type of interaction is farer reaching and may cover distances until more than 5 nm. Förster [28, 95] and Perrin [96, 97] established eq. (11) for the quantitative description of FRET where the rate constant of energy transfer (k_T) corresponds to the inverse sixth power of the distance R between the centers of the transition dipoles.

$$k_T = \frac{1000 \cdot (\ln 10) \cdot \kappa^2 \cdot J \cdot \Phi_D}{128 \cdot \pi^5 \cdot N_A \cdot \tau_D \cdot n^4 \cdot R^6} \tag{11}$$

J in eq. (11) is the overlap integral between the fluorescence spectrum of the energy donor and the absorption spectrum of the energy acceptor, Φ_D is the fluorescence quantum yield of the donor, N_A Avogadro's number, τ_D the fluorescence lifetime of the energy donor, and n the index of refraction.

$$\kappa = \cos\ (\theta_T) - 3\ \cos\ (\theta_D)\ \cos\ (\theta_A) \tag{12}$$

The geometry factor κ is a sum of scalar products and can be calculated with eq. (12) where θ_T is the angle between the electronic transition moments μ of D and A. θ_D is the angel between the transition moment of the donor and θ_A of the acceptor, respectively, and the interconnecting vector. The R^{-6} dependence of the rate of energy transfer is widely applied for the determination of inter and intra molecular distances such as a molecular ruler and obtained a special importance for biochemical investigation. The orientation factor κ^2 becomes 2/3 for mobile structures with tumbling chromophores as a consequence of integration over all orientations. Equation (11) is generally accepted; however, its practical application is still subject of considerations [98, 99]. As a consequence, we tested the applicability of eq. (11) where κ becomes zero for orthogonal transition moments between the donor and the acceptor if one of the transition moments is orthogonal to the interconnecting vector. As a consequence, both chromophores should be completely decoupled and operate independently such as with dual fluorescence.

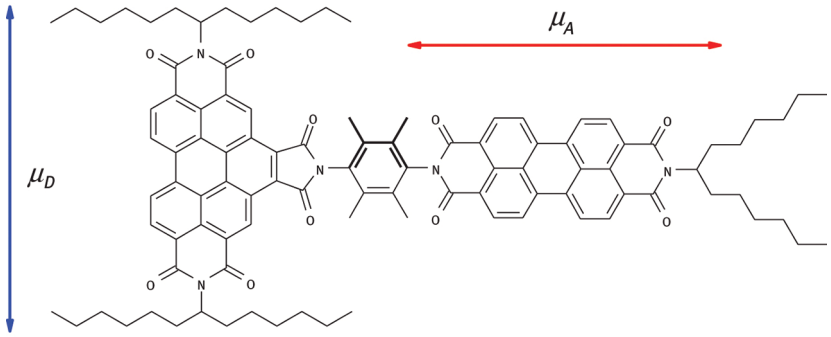

18

We prepared the dyes **18** for a test of eq. (11) [100] where the condition κ = 0 is fulfilled because the transition moment of the hypsochromically absorbing benzoperylene as the energy donor (blue vertical vector on the left) is orthogonal to the bathochromically absorbing perylene as the energy acceptor (red horizontal vector on the right); the interconnecting vector is orthogonal to the transition moment of the donor. As a consequence of κ = 0, energy transfer should be suppressed and independent fluorescence of both chromophores should be observed. In contrast to the theory, a fast and efficient energy transfer within 9.4 ps proceeded [101] with close to 100% fluorescence quantum yield for optical excitation of the fluorescence donor. The distance between the two orthogonal chromophores could be successively prolonged until 5 nm without inhibition of the energy transfer. An analysis of the rate of energy transfer as a function of the inter chromophore distance indicated the R^{-6} dependence as an only rough approximation [102]. Moreover, the overlap integral J in eq. (11) was successively diminished by means of the selection of suitable chromophores; however, no significant influence on the efficiency of energy transfer was found [103]. The unusual energy transfer was attributed to noise-induced processes with the contribution of molecular vibrations where this mechanism was supported by quantum chemical calculations [104, 105]. As a consequence, the well-established dipole–dipole interaction as the mechanism of FRET seems to be not the only way for a longer-distance energy transfer, but other ways with the contribution of molecular dynamics have to be considered, in particular for molecular geometric conditions with low valued of κ.

10 Charge transfer

Neighboring electron rich or electron depleted systems can induce electron transfer reaction of fluorescent chromophores where distances up to 5 nm may be spun for suitable chemical structures. The transfer of the energy rich electron means a photo-induced reduction where the water splitting and subsequent reduction of carbon

dioxide in photosynthesis [93] is the most prominent process. A photochemical oxidation is favored in less electron rich chromophores such as the here discussed perylenebiscarboximides with four electron withdrawing carbonyl groups and means a uptake of an electron by the photo-induced half vacant HOMO; see Figure 15. The transition probability of the electron transferred to the LUMO back to the substituent is so low that generally radiationless processes dominate and no fluorescence is observed. On the other hand, the direct optical excitation from the substituent into the LUMO can be observed with comparably low probability such as with a sulfur-containing heterocycle attached to the chromophore [64].

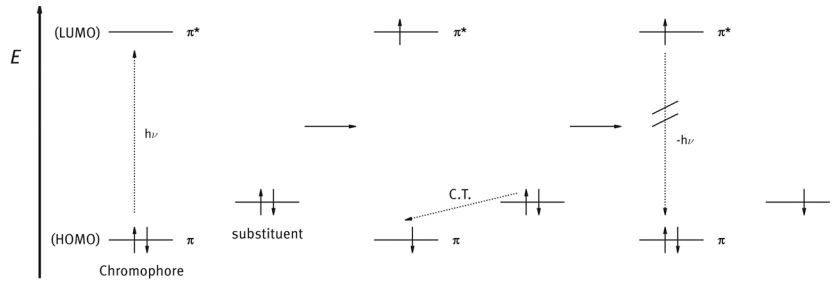

Figure 15: Photo oxidation of an electron rich, energetically high-lying substituent. The photo-induced half vacant HOMO is filled by an electron transfer from the substituent with the consequence of charge separation and fluorescence quenching.

The fluorescence quenching by electron and charge transfer reactions, respectively, was demonstrated with the perylene carboximide **19 (**RN 207394-04-5) [106], where the electron rich amino group is attached to the chromophore.

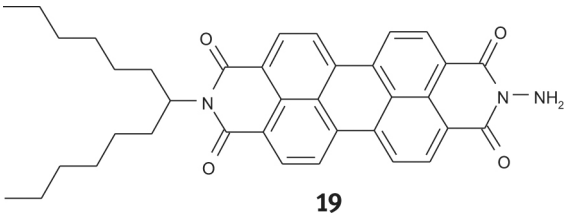

19

As a consequence, the fluorescence becomes quenched by an electron transfer from the amino group to the perylene chromophore [107]; the amino group is electronically decoupled from the chromophore because of orbital nodes in HOMO and LUMO at the linking nitrogen atom of the carboximide [108]. Some re-orientation in the electronically excited state of **19** seems to be important for this process [109]. This fluorescence quenching may be applied for analytical applications such as for the determination of aldehydes [110]. On the other hand, the electron transfer in Figure 15 causes a charge separation and may initiate photochemically induced reductions. The charge separation may proceed to other chromophores such as corroles [111, 112] or even by more distant colorless electron rich groups [113] where colorless local electron rich structures may be realized by the α-effect [114, 115]; this is given in isoxazolidines where a charge separation of 1.6 nm cold be induced [116].

11 Chemiluminescence

The S_1 state of dyes exhibits fluorescence in suitable chromophores where it is unimportant how the state was reached. The main topic of this contribution was the light-induced fluorescence; however, α-, β- or γ-radiation may cause the electronic excitation of dye molecules as well. Even chemical reactions may end-up in electronically excited states where the enforcing of symmetry forbidden reactions [117] by plenty of reaction enthalpy is an attractive way. This chemiluminescence is widely used in biochemistry [118, 119] because of sensitivity. The oxidation of Luminol (3-hydroxyphthalazine, RN 521-31-3) catalyzed by iron ions is a prominent example. Nature realized chemiluminescence, for example, in the firefly (*Photonius·Py*ralis) with the mechanism of Figure 16.

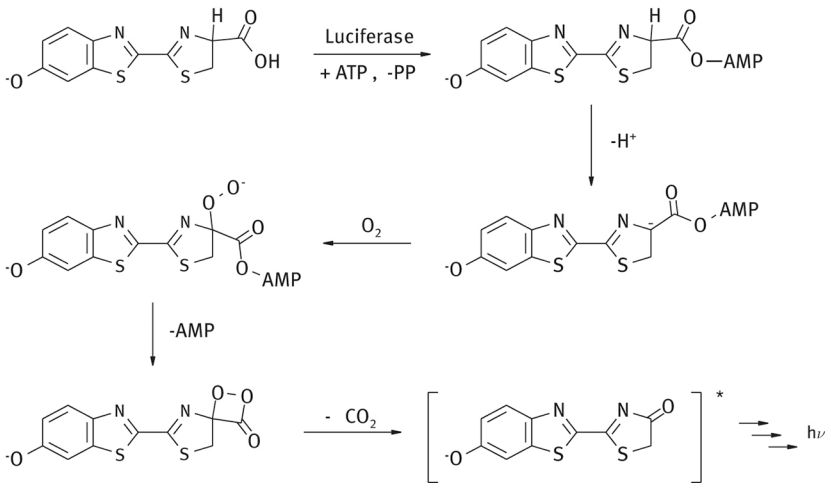

Figure 16: Chemical pathway for chemiluminescence in the firefly of Photonius Pyralis ($\eta = 88\%$).

The starting carboxylic acid is transferred in an energy consummating process enzymatically into the mixed anhydride with a derivative of diphosphoric acid. This increases the acidity of the α-proton of the carboxylic acid allowing a deprotonation with a subsequent autoxidation to the hydroperoxide anion. The strong α-effect nucleophile forms a dioxetanone derivative of the chromophore by intramolecular ring closure and loss of AMP. The symmetry forbidden ring scission leaves a neutral CO_2 and an optically excited chromophore that exhibits the nice green light of chemiluminescence. The staring carboxylic acid is recovered by enzymatic carboxylation and reduction as well as ATP from AMP.

Chemiluminescent emergency sticks operate with a similar mechanism where oxalic chloropheylesters are the staring material; Figure 17. The reaction with hydrogenperoxide and base give partial hydrolysis and subsequent ring closure with the anion of this strong α-effect nucleophile forming the dioxetanedione. The ring scission of the latter leaves a neutral CO_2 and one in the excited state. The fluorescence of CO_2 is weak; however, a sensitising of suitable fluorescent dyes results in bright chemiluminescent light [120, 121].

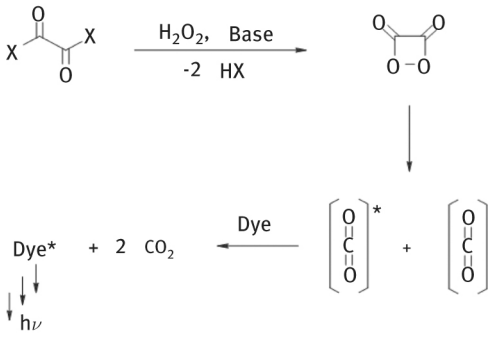

Figure 17: Oxalester chemiluminescence by sensitising fluorescent dyes.

Chemiluminescence is generally of interest in analytics for highly sensitive measurements because optical excitation is not necessary and thus, there is no interference by stray light.

12 Aggregation and fluorescence

The extended double bond systems in dyes, in particular large aromatic or hetero aromatic systems, exhibit strong dispersion interactions and the tendency of juxtaposing to form aggregates. This is favored in stronger polar media such as water. There are consequences for light absorption by such interactions; this is discussed by means of perylene dyes **1** and **10** ($n = 2$), respectively, because there is only one electronic transition moment in the visible parallel to the long axis of the chromophore; thus, there are clear conditions. One can distinguish between two significant basic types of geometric arrangements: (i) a co-planar sandwich-like orientation of the chromophores and the transition moments, respectively. Scheibe named this orientation *H*-aggregate because of hypsochromic shifts of the absorption [122]; see Figure 18, left blue curve and schematic indication of the transition moments down, within the curve.

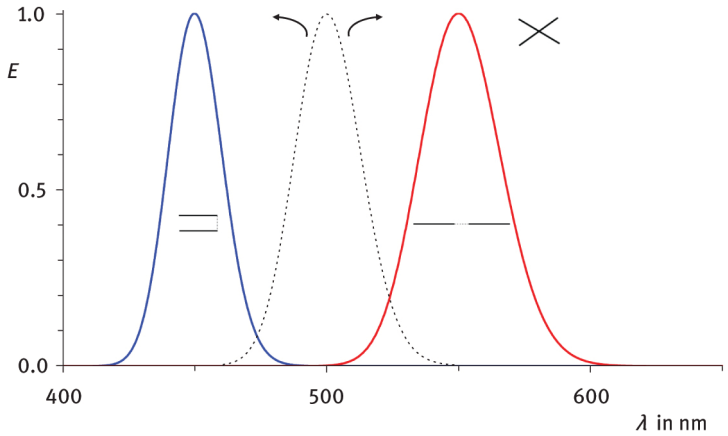

Figure 18: Schematic light absorption of a dye with the absorption maximum at 500 nm (black, dotted curve). Blue curve left: Hypsochromically shifted absorption by *H* aggregation and schematic indication of the transition moments down, within the curve. Red curve right: Bathochromically shifted absorption by *J* aggregation and schematic indication of the transition moments down, within the curve. Right, top: Schematic skew arrangement of the transition moments with hypsochromic and bathochromic absorption bands: Davydov splitting.

The movement of the significant electrons for electronic transitions becomes antiparallely synchronized in coplanar arrangements of aggregated **1** such as in polar media because of Coulomb interactions. As a consequence, charges proximate averaged more than in isolated chromophores causing a higher energy of electronic excitation and a more hypsochromic absorption, respectively (exciton interactions). This compact arrangement of molecular antennae diminish their effective lengths and decrease the molar absorptivity ε [123]. The coupled transition moment exhibits point symmetry for fluorescence where competing radiationless processes become dominant so that fluorescence will be quenched according Förster's analysis [124]. Such aggregation is favored with increasing of the chemical concentration of dyes in many cases. The consequences concerning suppressing fluorescence are known as concentration quenching. A linear arrangement (ii) causes a synchronous, parallel movement of the involved electrons and thus, a larger distance with even proximate opposite charges lowers the required energy of excitation and a bathochromic shift of the absorption, respectively; see Figure 18, right red curve and schematic arrangement of the transition moments down, within the curve. This type of aggregate is known as *J*- aggregates according to the discoverer Jelley [125]. An effective prolongation of the antenna causes an increase of the absorptivity ε [126]. There is also an increased transition moment for light emission where fluorescence of *J*-aggregates is observed; however, fluorescence quantum yields reach 20% only for few examples because of the lability of the arrangement. Such optical behavior is both observed for dimers and higher aggregates.

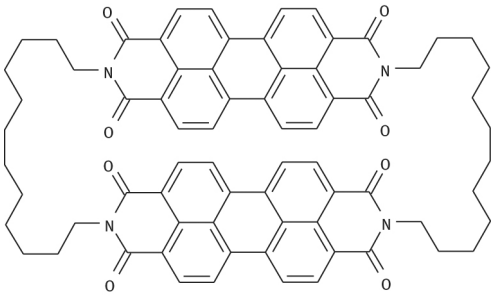

20

A skew arrangement of transition moments is schematically indicated in Figure 18, right top and allows both transitions. These are known as Davydov splitting [127]. A dominant *H* component can absorb light where the minor *J* component may be responsible for fluorescence (inner energy transfer). This could be realized for **1** in micells [128] or intramolecular with the more stable cyclophanes [129, 130].

The hypsochromically shifted absorption of the cyclophane **20** (RN 214078-84-9) [129] compared with **1** is shown in Figure 19 where the bathochromically shifted fluorescence causes an increased Stokes' shift. Cyclophanes of dyes may be efficiently synthesized by means of olefin metathesis [130].

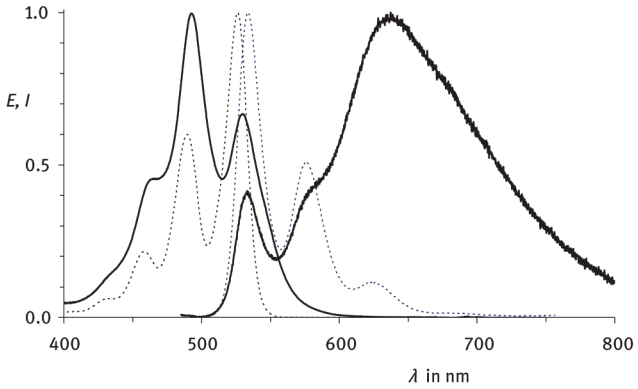

Figure 19: UV/Vis absorption (left) and fluorescence spectra (right) in chloroform. **20**: Thick solid curves compared with **1** (thin, dotted curves).

13 Optical impression of fluorescence

Fluorescent materials are of interest for special optical effects. The extinction E of a Gaussian curve of the schematic light absorption in Figure 2 was transformed to the residual light intensity I by passing of white light ($I_o = 1$ for any wavelengths) a sample with $E = 1$ at 500 nm is shown in Figure 20, left. There one can see the broad loss of intensity in the important region of high intensities because of the broad socket of the absorption. This makes the generation of clear colors difficult by means of absorbing dyes and means a problem for color print; for exact color metric see ref [131, 132].

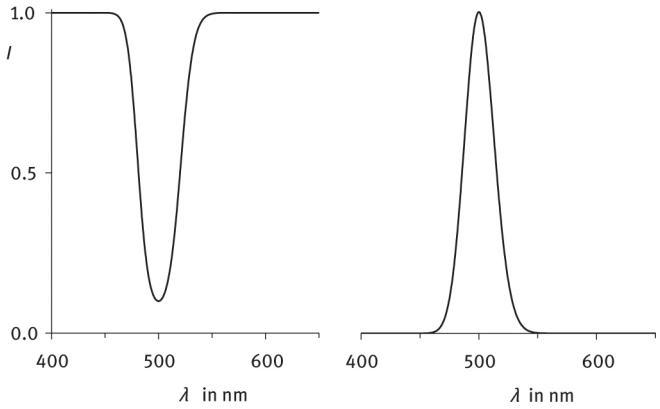

Figure 20: Schematic comparison of a typical spectral dependence of light intensity I. Left: Passing of white light with the Intensity $I_o = 1$ through a sample with the absorptivity $E = 1$ at 500 nm. Right: Same spectral dependence of fluorescence light with maximal intensity $I = 1$ at 500 nm.

The spectral intensity of a fluorescence band with the same parameters is opposite and results in a comparably slim maximum; Figure 20, right. As a consequence, very clear and deep colors, nearly like spectral colors, can be obtained. This is demonstrated by means of color metrics with the comparison of absorption and emission colors of a perylene derivative [79].

14 Closing remarks

Generally, fluorescence can be detected with high sensitivity and is of special interest for uncomplicated analytical methods. This is of special interest in biochemistry by coding the Green Fluorescent Protein (GFP). There is only a limitation to high concentration because of the tendency for aggregation. A linear dependence of the fluorescence intensity is given until very low concentrations, for less than picomolar [133] and even further until single molecules [134]. Absorbed light quanta should be re-emitted for such applications as efficiently as possible. However, they might also initiate various processes in suitable chemical structures. The temporary stored energy by the dyes in the order of some nanoseconds enables many possibilities because of possible induction of photo chemical processes, energy transfer even for molecular electronics, for light collection and for

single electron transfer where charge separation allows organic photovoltaics [135]. This can be controlled by means of molecular architecture [136] of suitable chemical structures. Structures for the transport of electrical charge are reaching resolutions as small as 5 nm in conventional electronics causing many technological problems because of the small size. The next steps of diminution of the active structure means molecular electronics where dyes such as **1** with a size of about 1 nm are attractive and would appreciably increase both the density of integration and frequency of cycle. The knowledge about the processes of fluorescence forms the basis for such developments.

References

[1] Raab W. Vorläufige Anzeige von der Entdeckung des Schillerstoffes, einer neuen vegetabilischen Substanz. Archiv f d ges Naturlehre. 1827;10:121–3.
[2] Rochleder F, Schwarz R. Über einige Bitterstoffe. Sitzungsberichte der k Akademie d Wiss Naturw Classe. 1852;9:70–9.
[3] Berzelius J. Jahres-Bericht über die Fortschritte der physischen Wissenschaften. Tübingen: Heinrich Laub Verlag, 1837:283–7.
[4] Nichols EL, Merritt E. Studies in luminescence, III. Phys Rev. 1904;19:18. DOI: 10.1103/PhysRevSeriesI.19.18. Chem Abstr. 1906:7432.
[5] Langhals H. Chromophores for picoscale optical computers. In: Sattler K editor, Fundamentals of picoscience, 705–27.Bosa Roca/US: Taylor & Francis Inc. CRC Press Inc, 2013. ISBN 13: 9781466505094, ISBN 10: 1466505095
[6] Bergmann L, Schaefer C. Lehrbuch der Experimentalphysik, Band 2, Elektromagnetismus: Elektromagnetismus. (W.Rath, co-author) Berlin: De Gruyter, 2015; ISBN: 9783110188981.
[7] Bergmann L, Schaefer C. Lehrbuch der Experimentalphysik / Optik. vol. 3. (H. Niedrig, ed.; W. Eichler, co-author) Berlin: De Gruyter, 2004; ISBN 978-3-11-017081-8.
[8] Langhals H. A re-examination of the line-shape of the electronic spectra of complex molecules in solution. Log-Normal Function Versus Gaussian. Spectrochim Acta Part A. 2000;56:2207–10.
[9] Langhals H. The rapid identification of organic colorants by UV/Vis-spectroscopy. Anal Bioanal Chem. 2002;374:573–8.
[10] Langhals H. UV-Visible spectroscopy and the potential of fluorescent probes. In: Frimmel FH, Refractory organic substances in the environment. Weinheim: Wiley-VCH, 2002:200–14. ISBN 3-527-30173-9.
[11] Langhals H, Ritter U. γ-hydroxyalkyl naphthalene-tetracarboxdiimides: Organic white pigments. Eur J Org Chem. 2008;3912–15.
[12] (a) Daubner SC, Fitzpatrick PF. Pteridines. Encyclopedia Biol Chem. (Eds.: W. J. Lennarz, M. D. Lane) 2004;3:556–60; Chem Abstr. 2005;143:55015; (b) Oliphant LW, Hudon J. Pteridines as reflecting pigments and components of reflecting organelles in vertebrates. Pigm Cell Res. 1993;6:205–8; Chem Abstr. 1994;120:159184; (c) Ziegler I. Pterins: pigments, cofactors and signal connection in cellular interaction. Naturwissenschaften. 1987;74:563–72; (d) Pfleiderer W, Natural pteridines – a chemical hobby. Adv Experim Med Biol. 1993;338:1–16; ISSN 0065–2598; (e) Landymore AF, Antia NJ, White-light promoted degradation of leucopterin and related pteridines dissolved in seawater, with evidence for involvement of complexation from major divalent cations of seawater. Marine Chem. 1978;6:309–25; Chem Abstr. 1978;89:220590.
[13] Bugnon P, Karrer K, Hahn M, Sieber W. (Ciba Specialty Chemicals Holding Inc., Switzerland). PCT Int Appl. WO 2006003093 (30.6.2004); Chem Abstr. 2006;144:109847.
[14] Langhals H, Eberspächer M. Water nanomicellar solutions naphthalenetetracarboxilic acid bisimides used as sunscreens. Ger Offen. DE 102013014353.5 27 Aug 2013, Ger Offen DE 102014012594 26 Mar 2015; Chem Abstr. 2015;162:454180.
[15] Rohn W. Anomale Dispersion einiger organischer Farbstoffe. Ann Phys. 1912;38:987–1013. DOI: https://doi.org/10.1002/andp.19123431007.
[16] Kuhn W. The physical significance of optical rotary power. Trans Faraday Soc. 1930;26:293–308. DOI: 10.1039/TF9302600293.
[17] Kirkwood JG. On the theory of optical rotatory power. J Chem Phys. 1937;5:479–421.
[18] Roduner E, Krüger T, Forbes P, Kress K. Optical spectroscopy. Fundamentals and advanced applications. London: World Scientific, Publishing Europe Ltd, 2019: ISBN 978-1-78634-610-0.
[19] Langhals H The determination of overlap between UV/Vis absorption and fluorescence spectra' Ber Bunsenges Phys Chem 1979;83:730–2.
[20] Langhals H, Eberspächer M, Hofer A. Learning about structural and optical properties of organic compounds through preparation of functional nano micelles while avoiding hazardous chemicals or complicated apparatus. J Chem Educ. 2015;92:1725–9. DOI: http://dx.doi.org/10.1021/acs.jchemed.5b00145.
[21] Wolfbeis OS. ed. Fluorescence Spectroscopy. New methods and applications. Berlin: Springer Verlag, 1993:ISBN 3-540-55281-2.
[22] http://www.cup.lmu.de/oc/langhals/S-13/S-13data.html.
[23] (a) Rothammel K. Antennenbuch. 5th edn. Stuttgart: Telekosmos Verlag, 1976. (b) Rüdenberg R. Der Empfang elektrischer Wellen in der drahtlosen Telegraphie. Ann d Phys. 1908;330:446–6. (c) Rüdenberg R. Der Empfang elektrischer Wellen in der drahtlosen Telegraphie. Ann d Phys Leipzig. 1908;25:466–500.
[24] McCoy EF, Ross IG. Electronic states of aromatic hydrocarbons: The Franck-Condon principle and geometries in excited states. Aust J Chem. 1962;15:573–90.
[25] Schmidt W. Optische Spektroskopie. 2nd ed. Weinheim: Wiley-VCH, 2000:ISBN 3-527-29828-2.
[26] Hund F. Zur Deutung der Molekelspektren III. Zeitschrift für Physik. 1927;43:805–26.
[27] Strickler SJ, Berg RA. Relationship between absorption intensity and fluorescence lifetime of molecules. J Chem Phys. 1962;37:814–22.
[28] Förster T. Fluoreszenz organischer Verbindungen. Göttingen: Vandenhoeck & Ruprecht, 1951:158.
[29] Schlücker T, Dhayalan V, Langhals H, Sämann C, Knochel P. Soluble adamantyl-substituted oligothiophenes with short fluorescence decay: An approach for ultra fast optical signal processing. Asian J Org Chem. 2015;4:763–9. DOI: 10.1002/ajoc.201500150.

[30] Langhals H. A concept for molecular addressing by means of far-reaching electromagnetic interactions in the visible. J Electr Electron Syst. 2017;215. DOI: http://dx.doi.org/10.4172/2332-0796.1000215.
[31] Hecht E. Optik. München: Oldenbourg, 2009. ISBN: 978-3-486-58861-3.
[32] Periasamy A, Clegg RM. Flim microscopy in biology and medicine. Boca Raton, Fla.: CRC Press, 2010. ISBN 978-1-4200-7890-9.
[33] Lewis GN, Calvin M. The color of organic substances. Chem Rev. 1939;25:273–328.
[34] Baeyer A. Ueber eine neue Klasse von Farbstoffen. Ber Dtsch Chem Ges. 1871;4:555–8.
[35] König W. Ueber den Begriff der "Polymethinfarbstoff" und eine davon ableitbare allgemeine Farbstoff -Formel als Grundlage einer neuen Systematik der Farbenchemie'. J Prakt Chem. 1926;112:1–36.
[36] Wiese WL. Atomic oscillator strengths for light elements - progress and problems. J Korean Phys Soc. 1998;33:207–13.
[37] Liu Y. A new method for obtaining Russell-Saunders terms'. J Chem Educ. 2011;88:295–8.
[38] Ludvíková L, Friš P, Heger D, Šebej P, Wirza J, Klán P. Photochemistry of rose bengal in water and acetonitrile: A comprehensive kinetic analysis'. Phys Chem Chem Phys. 2016;18:16266–73.
[39] Berlman IB. Handbook of fluorescence spectra of aromatic molecules, New York: Academic Press, 1971. LCCC-Nr. 78–154388.
[40] Sauer M, Hofkens J, Enderlein J. Handbook of fluorescence spectroscopy and imaging. Weinheim: Wiley VCH, 2011: ISBN 978-3-527-31669-4.
[41] Krasowitzkii BM, Bolotin BM. Organic luminescent materials, Weinheim: Wiley-VCH, 1988: ISBN 3-527-26728-X.
[42] https://www.aatbio.com/resources/quantum-yield/. 15 Jan 2020.
[43] Christie RM. Fluorescent dyes. Rev Prog Coloration. 1993;23:1–18.
[44] Langhals H, Jaschke H. Naphthalene amidine imide dyes by transamination of naphthalene bisimides. Chem Eur J. 2006;12:2815–24.
[45] Langhals H, Ritter U. γ-hydroxyalkyl naphthalene-tetracarboxdiimides: Organic white pigments. Eur J Org Chem. 2008;3912–15.
[46] Langhals H, Eberspächer M. Water nanomicellar solutions naphthalenetetracarboxilic acid bisimides used as sunscreens. Ger Offen. DE 102014012594.7 27 Aug 2014. Chem Abstr. 2015;162:454180.
[47] Adachi M, Murata Y, Nakamura S. Spectral similarity and difference of Naphthalenetetracarboxylic dianhydride, perylenetetracarboxylic dianhydride, and their derivatives. J Phys Chem. 1995;99:14240–6.
[48] Zollinger H. Color chemistry: Syntheses, properties, and applications of organic dyes and pigments. Zürich: Verlag Helvetica Chimica Acta, 2003:ISBN 10: 3906390233 ISBN 13: 9783906390239.
[49] Hunger K, Schmidt MU, Heber T, Reisinger F, Wannemacher S. Industrial organic pigments: production, crystal structures, properties, applications. 4th ed. Weinheim: Wiley-VCH, 2018:ISBN 978-3-527-32608-2.
[50] Langhals H. Primary methods of generating solar power by using the targeted modification of fluorescent systems. Habilitationsschrift, Albert-Ludwigs-Universität Freiburg 1981, translation 9 Aug 2019. DOI: https://doi.org/10.5282/ubm/epub.68484.
[51] Graser F, Feichtmayr F. Perylenetetracarboxylic acid diimide dyes. Eur Pat Appl. 1982;97, 7 July 1982. EP 55363 A1 19820707. Chem Abstr.218033.
[52] https://www.cup.lmu.de/oc/langhals/Perylenebiscarboximides/index.html. 15 Jan 2020.
[53] Langhals H, Demmig S, Potrawa T. The relation between packing effects and solid state fluorescence of dyes. J Prakt Chem. 1991;333:733–48.
[54] Langhals H, Karolin J, Johansson LB. Spectroscopic properties of new and convenient standards for measuring fluorescence quantum yields. J Chem Soc Faraday Trans. 1998;94:2919–22.
[55] Langhals H, El-Shishtawy R, von Unold P, Rauscher M. Methoxyperylene bisimides and perylene lactame imides: novel, red fluorescent dyes. Chem Eur J. 2006;12:4642–5. supporting information.
[56] Langhals H, Walter A, Rosenbaum E, Johansson LB. A versatile standard for bathochromic fluorescence based on intramolecular FRET. Phys Chem Chem Phys. 2011;13:11055–9.
[57] Langhals H, Schönmann G, Feiler L. A two-step synthesis of quaterrylenetetracarboxylic bisimides - novel NIR fluorescent dyes. Tetrahedron Lett. 1995;36:6423–4.
[58] Langhals H, Büttner J, Blanke P. A two-step synthesis for quarterrylene bisimides. Application of the "green route" method. Synthesis. 2005;364–6.
[59] Langhals H, Zgela D, Lüling R. Sexterrylenetetracarboxylic bisimides: NIR dyes. J Org Chem. 2015;80:12146–50. DOI: 10.1021/acs.joc.5b02092.
[60] Schweizer HR. Künstliche organische Farbstoffe und ihre Zwischenprodukte, Berlin: Springer-Verlag, 1964:LCCC Nr. 63–23133.
[61] Stauble M, Weber K. *peri*-Dicarboxylic acid imide dyes. CIBA Ltd., US patent US 2914531 19591124 Chem Abstr. 1960;54:47263.
[62] Syebold G, Wagenblast G. New perylene and violanthrone dyestuffs for fluorescent collectors. Dyes Pigm. 1989;11:303–17.
[63] Langhals H, Christian S, Hofer A. The substitution of aromatics by amines at room temperature with negative energy of activation: Amino peri-arylenes as metal-free components for dye-sensitized solar cells. J Org Chem. 2013;78:9883–91.
[64] Langhals H, Kirner S. Novel fluorescent dyes by the extension of the core of perylene-tetracarboxylic bisimides. Eur J Org Chem. 2000;365–80.
[65] Langhals H, Jaschke H, Ring U, von Unold P. Imidazolo perylene imides: A highly fluorescent and stable replacement of terrylene. Angew Chem. 1999;111:143–5. Angew. Chem. Int. Ed. Engl. 1999;38:201–3.
[66] Langhals H. Primary methods of generating solar power by using the targeted modification of fluorescent systems, Habilitationsschrift, Albert-Ludwigs-Universität Freiburg. 1981. Open Access LMU UB München 15 Jan 2020. DOI: https://doi.org/10.5282/ubm/epub.68484.
[67] Schäfer FP, Drexhage KH. Dye lasers. Berlin: Springer-Verlag, 1977: ISBN 978-3-540-51558-6.
[68] Bogert MT, Renshaw RR. 4-Amino-*o*-phthalic acid and some of its derivatives. J Am Chem Soc. 1908;30:1135–44.
[69] Fritzsche K, Langhals H. Elektronenreiche Heterocyclen als Donorgruppen in Fluoreszenzfarbstoffen. Chem Ber. 1984;117:2275–86.
[70] Zhmyreva IA, Zelinskii VV, Kolobkov VP, Krasnitskaya ND. Universal scale for the action of solvents on the electron spectra of organic compounds. Dokl Akad Nauk SSSR. 1959;129:1089–92. Chem Abstr. 1961; 55:141336.
[71] Langhals H. Heterocyclic structures applied as efficient molecular probes for the investigation of chemically important interactions in the liquid phase. Chem Heterocycl Compd. 2017;53:2–10. DOI: 10.1007/s10593-017-2014-z.

[72] Langhals H. 'Polarität von organischen Gläsern. Angew Chem. 1982;94:452–3. Angew Chem Int Ed Engl. 1982;21:432–433.
[73] Potrawa T, Langhals H. Fluoreszenzfarbstoffe mit großen Stokes-Shifts - lösliche Dihydropyrrolopyrroldione. Chem Ber. 1987;120:1075–8.
[74] Langhals H, Greiner R, Schlücker T, Jakowetz A. Light-driven molecular dynamics in perylenes with medium-controlled emission. J Org Chem. 2019; 84: 5425–30. https://pubs.acs.org/doi/pdf/10.1021/acs.joc.9b00409.
[75] Haberhauer G, Gleiter R, Burkhart C. Planarized intramolecular charge transfer: A concept for fluorophores with both large stokes shifts and high fluorescence quantum yields. Chem Eur J. 2016;22:971–8.
[76] Lewis GN, Calvin M. The color of organic substances. Chem Rev. 1939;25:273–328.
[77] Langhals H, Unold PV. Tetracarboxylic Bisimide-lactame-ring-contractions: A novel type of rearrangement. Angew Chem. 1995;107:2436–9. Angew Chem Int Ed. 1995;34:2234–2236.
[78] Rettig W. Charge separation in excited states of decoupled systems: Twisted intramolecular charge transfer (TICT) compounds and implications for the development of new laser dyes and for the primary process of vision and photosynthesis. Angew Chem. 1986;98:969–86. Angew Chem Int Ed. 1986;25:971–988.
[79] Greiner R, Schlücker T, Zgela D, Langhals H. Fluorescent aryl naphthalene dicarboximides with large Stokes' shifts and strong solvatochromism controlled by dynamics and molecular geometry. J Mater Chem C. 2016;4:11244–52. DOI: 10.1039/C6TC04453K.
[80] Tietze E, Bayer O. Sulfonic acids of pyrene and their derivatives. Justus Liebigs Ann Chem. 1939;540:189–210.
[81] Förster T, Völker S. Laser-excited absorption spectroscopy of rapid proton transfer processes. II. Reactions with weak acids. Zeitschr Phys Chem (München, Germany). 1975;97:275–84. Chem Abstr 1976; 84:104801:.
[82] Langhals H, Rauscher M. NIR absorption of perylene dyes and fluorescence with large Stokes shift by simple deprotonation. Z Naturforsch. 2013;68b:683–6.
[83] Vogt LH, Jr., Wirth JG. Crystal and molecular structure of 2,2′-bis(6-methyl-3-pyridinol). J Am Chem Soc. 1971;93:5402–5.
[84] Langhals H, Pust S. Fluoreszenzfarbstoffe mit großen Stokes-Shifts - eine einfache Synthese von (2,2′-Bipyridin)-3,3′-diol. Chem Ber. 1985;118:4674–81.
[85] Bulska H. Intramolecular cooperative double proton transfer in [2,2′-bipyridyl]-3,3′-diol. Chem Phys Lett. 1983;98:398–402.
[86] Naumann C, Langhals H. A simple synthesis of Dihydroxybipyridyls. Synthesis. 1990;279–81.
[87] Johansson LB, Persson L, Langhals H. Conspicuous absorption and fluorescence spectroscopic properties of 3,3′-dihydroxy-2,2′-bipyridines in solution. J Chem Soc Faraday Trans. 1996;92:4909–11.
[88] Stock K, Schriever C, Lochbrunner S, Riedle E. Reaction path dependent coherent wavepacket dynamics in excited state intramolecular double proton transfer. Chem Phys. 2008;349:197–203.
[89] Plasser F, Barbatti M, Aquino AJ, Lischka H. Excited-state diproton transfer in [2,2′-bipyridyl]-3,3′-diol: The mechanism Is sequential, not concerted. J Phys Chem A. 2009;113:8490–9.
[90] Zhao J, Liu X, Zheng Y. Controlling excited state single versus double proton transfer for 2,2′-bipyridyl-3,3′-diol: Solvent effect. J Phys Chem A. 2017;121:4002–8.
[91] Reynal A, Etxebarria J, Nieto N, Serres S, Palomares E, Vidal-Ferran A. A bipyridine-based "naked-eye" fluorimetric Cu^{2+} chemosensor. Europ J Inorg Chem. 2010;1360–5.
[92] Valeur B, Berberan-Santos M. Excitation energy transfer. Molecular fluorescence: Principles and applications. 2nd ed. Weinheim: Wiley-VCH, 2012. DOI: 10.1002/9783527650002.ch8. ISBN 9783527328376.
[93] Golbeck JH. Structure and function of photosystem I. Annual Rev Plant Physiol Plant Mol Biol. 1992;43:293–324.
[94] Dexter DL. A theory of sensitized luminescence in solids. J Chem Phys. 1953;21:836–50.
[95] Förster T. Zwischenmolekulare Energiewanderung und Fluoreszenz. Ann Phys. 1948;437:55–75. https://doi.org/10.1002/andp.19484370105.
[96] Perrin F. The fluorescence of solutions: Molecular induction, polarization and duration of emission and photochemistry. Ann Phys. [10]. 1929;12:169–275. Chem Abstr 1930;24:0.25377.
[97] Perrin F. Activation by light and by collisions in thermal equilibrium. Chem Rev. 1930;7:231–7. Chem Abstr 1930; 24:34772.
[98] VanBeek DB, Zwier MC, Shorb JM, Krueger BP. Fretting about FRET: Correlation between κ and *R*. Biophy J. 2007;92:4168–78.
[99] Muñoz-Losa A, Curutchet C, Krueger BP, Hartsell LR, Mennucci B. Fretting about FRET: Failure of the ideal dipole approximation. Biophys J. 2009;96:4779–88.
[100] Langhals H, Poxleitner S, Krotz O, Pust T, Walter A. FRET in orthogonally arranged chromophores. Eur J Org Chem. 2008;4559–62.
[101] Langhals H, Esterbauer AJ, Walter A, Riedle E, Pugliesi I. Förster resonant energy transfer in orthogonally arranged chromophores. J Am Chem Soc. 2010;132:16777–82.
[102] Nalbach P, Pugliesi I, Langhals H, Thorwart M. Noise-induced Förster resonant energy transfer between orthogonal dipoles in photoexcited molecules. Phys Rev Lett. 2012;108:218302–1–218302-5.
[103] Langhals H, Walter A. FRET in dyads with orthogonal ohromophores and minimal spectral overlap. 2019. submitted.
[104] Renger T, Dankl M, Klinger A, Schlücker T, Langhals H, Müh F. Structure-based theory of fluctuation-induced energy transfer in a molecular dyad. J Phys Chem Lett. 2018;9:5940–7. DOI: 10.1021/acs.jpclett.8b02403.
[105] Václav P, Sláma V, Lincoln CN, Langhals H, Riedle E, Mančal T, et al. Geometric dependencies of vibronically mediated excitation transfer in rylene dyads. arXiv.org, e-Print Archive, Physics. 2018:1–8. https://arxiv.org/pdf/1808.02467.pdf.
[106] Langhals H, Jona W. Intense dyes through chromophore-chromophore Interactions: Bi- and trichromophoric perylene-3,4:9,10-bis(dicarboximide)s. Angew Chem. 1998;110:998–1001. Angew Chem Int Ed. 1998;37:952–955.
[107] Langhals H, Jona W. Identification of carbonyl compounds by fluorescence: A novel carbonyl derivating reagent. Chem Eur J. 1998;4:2110–16.
[108] Langhals H, Demmig S, Huber H. Rotational barriers in perylene fluorescent dyes. Spectrochim Acta. 1988;44A:1189–93.
[109] Langhals H, Riedle E, de Vivie-riedle R. unpublished results. 2011.
[110] Mohr GJ, Spichiger UE, Jona W, Langhals H. Using *N*-aminoperylene-3,4:9,10-tetracarboxyl-bisimide as a fluorogenic reactand in the optical sensing of aqueous propionaldehyde. Anal Chem. 2000;72:1084–7.

[111] Tasior M, Gryko DT, Shen J, Kadish KM, Becherer T, Langhals H, et al. Energy- and electron-transfer processes in corrole-perylenebisimide-diphenylacetylene array. J Phys Chem C. 2008;112:19699–709.
[112] Flamigni L, Ciuciu AI, Langhals H, Böck B, Gryko DT. Improving the photoinduced charge separation parameters in corrole-perylene carboximide dyads by tuning the redox and spectroscopic properties of the components. Chem an Asian J. 2012;7:582–92.
[113] Flamigni L, Ventura B, Barbieri A, Langhals H, Wetzel F, Fuchs K, et al. On/Off switching of the perylene tetracarboxylic bisimide luminescence by means of substitution at the N position by electron rich mono-, di- and tri-methoxybenzenes. Chem Eur J. 2010;16:13406–16.
[114] Dessolin M. Reactivity of α-effect nucleophiles toward aryl acetates. Effect of substituent in leaving groups. Tetrahedron Lett. 1972;45:4585–8.
[115] Liebman JF, Pollack RM. Aromatic transition states and the α effect. J Org Chem. 1973;38:3444–545.
[116] Langhals H, Obermeier A, Floredo Y, Zanelli A, Flamigni L. Light-driven charge separation in isoxazolidine-perylene bisimide dyads. Chem Eur J. 2009;15:12733–44.
[117] Woodward RB, Hoffmann R. The conservation of orbital symmetry. Angew Chem Int Ed. 1969;8:781–853.
[118] Roda A. Chemiluminescence and Bioluminescence. Cambridge: Royal Society of Chemistry, 2011. ISBN 978-1-84755-812-1.
[119] Brolin S, Wettermark G. Bioluminescence analysis, Weinheim: Wiley-VCH, 1992. ISBN 3-527-28194-0.
[120] van Moer A, Ladyjensky J. Chemiluminescent solution based on substituted perylene. Eur Pat Appl. 1990;EP 403809 A2 19901227. Chem Abstr. 1991;114:256680.
[121] Nowak B, Ladyjensky J. Multi-color chemiluminescent lighting device and method of making same. *US Patent* U.S. (1996), US 5508893 A 19960416. Chem Abstr. 1996;125:21964.
[122] Scheibe G. Variability of the absorption spectra of some sensitizing dyes and its cause. Angew Chem. 1936;49:563.
[123] Langhals H. Handling electromagnetic radiation beyond terahertz using chromophores to transition from visible light to petahertz technology. J Electric Electron Syst. 2014;3:125.
[124] Förster T. Energiewanderung und Fluoreszenz. Naturwissenschaften. 1946;33:166–75.
[125] Jelley EE. Spectral absorption and fluorescence of dyes in the molecular state. Nature. 1936;138:1009–10.
[126] Langhals H, Jona W. Intense dyes through chromophore - chromophore Interactions: Bi- and trichromophoric Perylene-3,4:9,10-bis(dicarboximide)s. Angew Chem. 1998;110:998–1001. Angew Chem Int Ed Engl. 1998;37:952–955.
[127] Davydow AS. Theory of molecular excitations, Transl. H. Kasha und M. Oppenheimer, Jr., New York: McGraw-Hill, 1962.
[128] Langhals H, Pust T. Lipophilic optical supramolecular nano devices in the aqueous phase. Green Sustainable Chem. 2011;1:1–6.
[129] Langhals H, Ismael R. Cyclophanes as model compounds for permanent, dynamic aggregates - induced chirality with strong CD effects. Eur J Org Chem. 1998;1915–17.
[130] Langhals H, Rauscher M, Mayer P. A sustainable preparation of functional perylenophanes by domino metathesis. Green Sustainable Chem. 2019;9:38–77.
[131] Chamberlin GJ, Chamberlin DG. Colour, Its measurement, computation and application, London: Heyden & Sons Ltd, 1980. ISBN 0-85501-222-6.
[132] Richter M. Einführung in die Farbmetrik, 2nd ed. Berlin: de Gruyter, 1981:ISBN 3-11-008209-8.
[133] Aubert C, Fünfschilling J, Zschokke-Gränacher I, Langhals H. Hochempfindliches Nachweisverfahren auf der Basis der Fluorescenz durch Laser-Anregung. Zeitschr Analyt Chem. 1985;320:361–4.
[134] Renge I, Hubner CG, Renn A, Langhals H, Wild UP. Slow photochemical transformations of single dye molecules in polymer environment at room temperature. J Lumines. 2002;98:91–6.
[135] Günes S, Neugebauer H, Sariciftci NS. Conjugated polymer-based organic solar cells. Chem Rev. 2007;107:1324—38.
[136] Langhals H, Saulich S. Bichromophoric perylene derivatives: Energy transfer from non fluorescent chromophores. Chem Eur J. 2002;8:5630–43.